

*Origin and geodynamic relationships of  
the Late Miocene to Quaternary alkaline  
basalt volcanism in the Pannonian basin,  
eastern–central Europe*

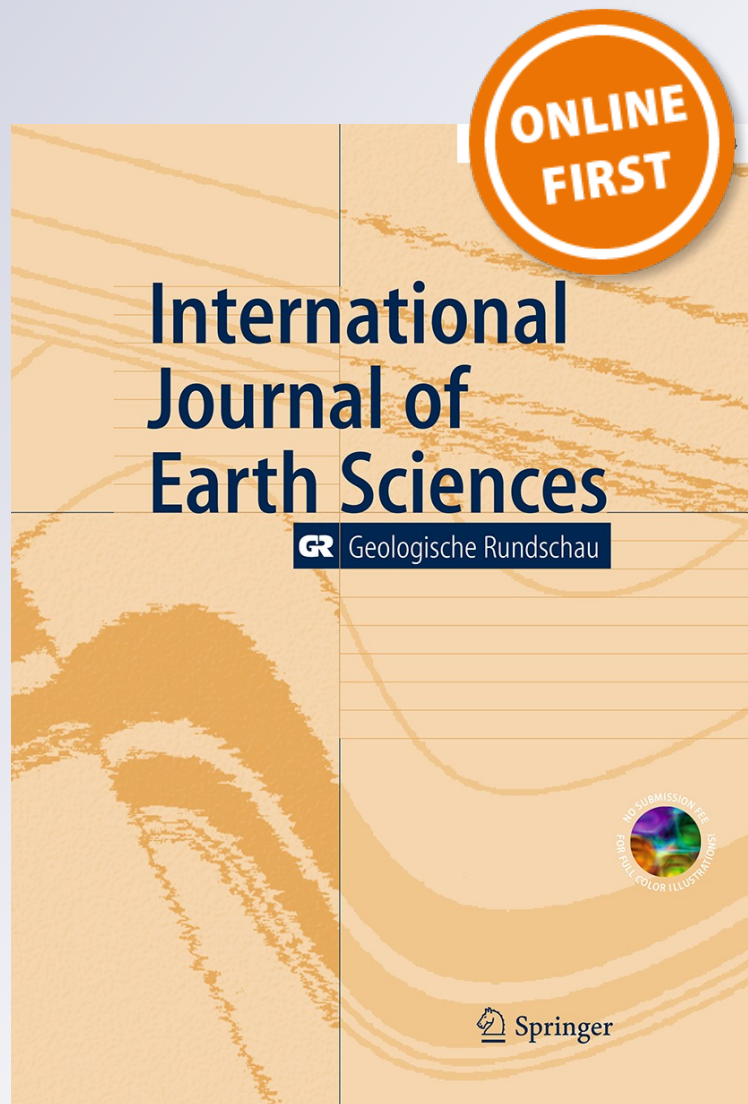
**Szabolcs Harangi, M. Éva Jankovics,  
Tamás Sági, Balázs Kiss, Réka Lukács &  
Ildikó Soós**

**International Journal of Earth  
Sciences**

GR Geologische Rundschau

ISSN 1437-3254

Int J Earth Sci (Geol Rundsch)  
DOI 10.1007/s00531-014-1105-7



**Your article is protected by copyright and all rights are held exclusively by Springer-Verlag Berlin Heidelberg. This e-offprint is for personal use only and shall not be self-archived in electronic repositories. If you wish to self-archive your article, please use the accepted manuscript version for posting on your own website. You may further deposit the accepted manuscript version in any repository, provided it is only made publicly available 12 months after official publication or later and provided acknowledgement is given to the original source of publication and a link is inserted to the published article on Springer's website. The link must be accompanied by the following text: "The final publication is available at [link.springer.com](http://link.springer.com)".**

# Origin and geodynamic relationships of the Late Miocene to Quaternary alkaline basalt volcanism in the Pannonian basin, eastern–central Europe

Szabolcs Harangi · M. Éva Jankovics · Tamás Sági ·  
Balázs Kiss · Réka Lukács · Ildikó Soós

Received: 18 March 2014 / Accepted: 9 November 2014  
© Springer-Verlag Berlin Heidelberg 2014

**Abstract** Alkaline basaltic volcanism has been taking place in the Carpathian–Pannonian region since 11 Ma and the last eruptions occurred only at 100–500 ka. It resulted in scattered low-magma volume volcanic fields located mostly at the margins of the Pannonian basin. Many of the basalts have compositions close to those of the primitive magmas and therefore can be used to constrain the conditions of the magma generation. Low-degree (2–3 %) melting could occur in the convective asthenosphere within the garnet–spinel transition zone. Melting started at about 100 km depth and continued usually up to the base of the lithosphere. Thus, the final melting pressure could indicate the ambient lithosphere–asthenosphere boundary. The asthenospheric mantle source regions of the basalts were heterogeneous, presumably in small scale, and included either some water or pyroxenite/eclogite lithology in addition to the fertile to slightly depleted peridotite. Based on the prevailing estimated mantle potential temperature (1,300–1,400 °C) along with the number of further

observations, we exclude the existence of mantle plume or plume fingers beneath this region. Instead, we propose that plate tectonic processes controlled the magma generation. The Pannonian basin acted as a thin spot after the 20–12 Ma syn-rift phase and provided suction in the sub-lithospheric mantle, generating asthenospheric flow from below the adjoining thick lithospheric domains. A near-vertical upwelling along the steep lithosphere–asthenosphere boundary beneath the western and northern margins of the Pannonian basin could result in decompressional melting producing low-volume melts. The youngest basalt volcanic field (Perşani) in the region is inferred to have been formed due to the dragging effect of the descending lithospheric slab beneath the Vrancea zone that could result in narrow rupture at the base of the lithosphere. Continuation of the basaltic volcanism cannot be excluded as inferred from the still fusible condition of the asthenospheric mantle. This is reinforced by the detected low-velocity seismic anomalies in the upper mantle beneath the volcanic fields.

**Electronic supplementary material** The online version of this article (doi:10.1007/s00531-014-1105-7) contains supplementary material, which is available to authorized users.

S. Harangi (✉) · M. É. Jankovics · T. Sági · B. Kiss · R. Lukács · I. Soós  
MTA-ELTE Volcanology Research Group, Pázmány sétány 1/C,  
1117 Budapest, Hungary  
e-mail: szabolcs.harangi@geology.elte.hu

S. Harangi · T. Sági  
Department of Petrology and Geochemistry, Eötvös University,  
Pázmány sétány 1/C, 1117 Budapest, Hungary

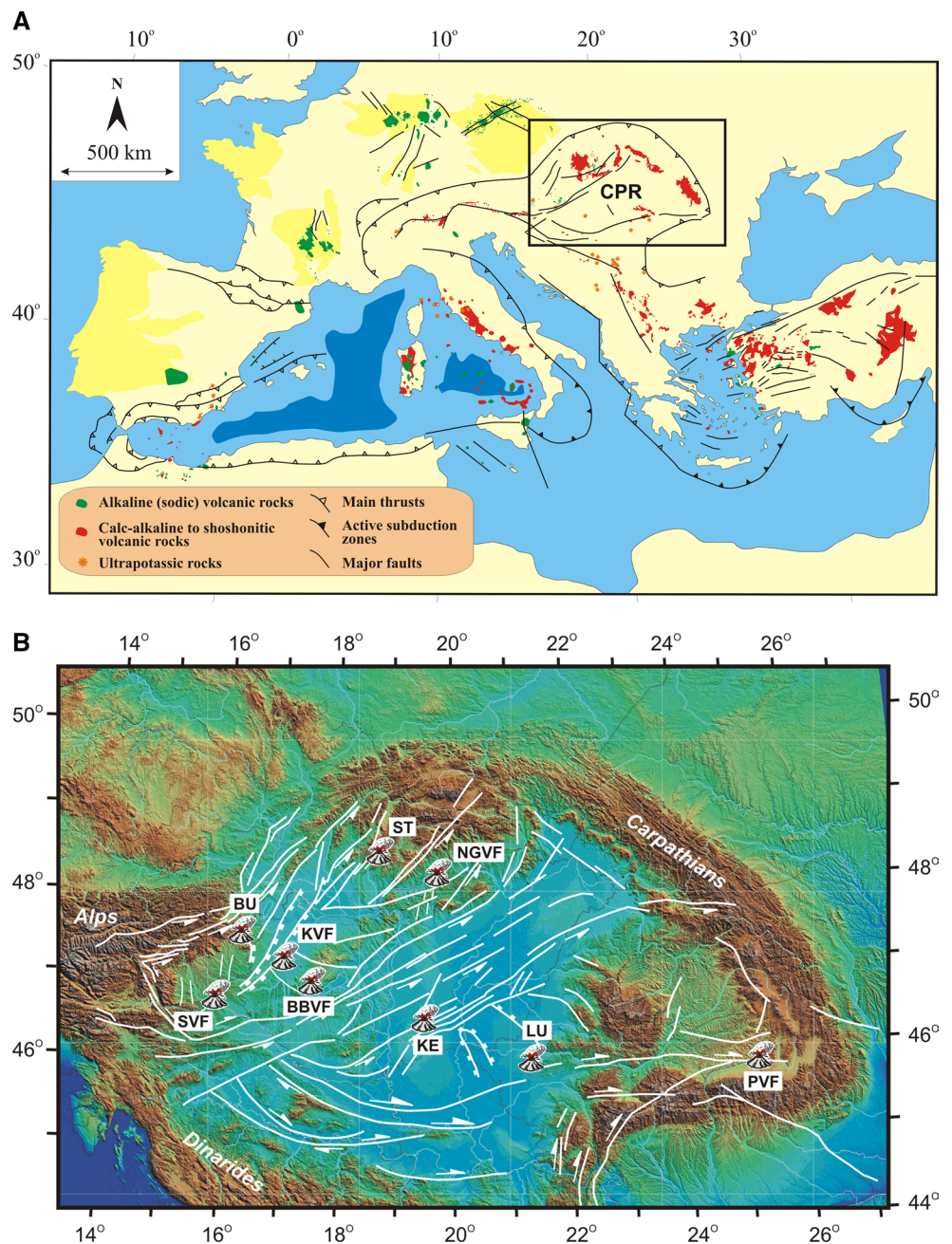
M. É. Jankovics · B. Kiss · R. Lukács  
Vulcano Research Group, Department of Mineralogy,  
Geochemistry and Petrology, University of Szeged,  
Egyetem utca 2, 6722 Szeged, Hungary

**Keywords** Basalt · Spinel · Carpathian–Pannonian region · Magma genesis · Monogenetic volcanic field · Asthenosphere flow

## Introduction

Origin of the basaltic magmas in monogenetic volcanic fields is a key issue to understand the nature of low-magma-flux, episodic, but long-lasting volcanic activity (Connor and Conway 2000; Wang et al. 2002; Aldanmaz et al. 2006; Jung et al. 2006, 2012; Valentine and Perry 2007; Blondes et al. 2008; Haase and Renno 2008; Brenna et al. 2012; McGee et al. 2013). Each volcano in such volcanic system is considered to represent eruption of a discrete magma

**Fig. 1** **a** Geological setting and **b** location of the Miocene to Quaternary basalts in the Carpathian–Pannonian region with the main tectonic lines (after Horváth et al. 2006). *SVF* Styrian Volcanic Field, *BU* Burgenland basalts, *KVF* Keme­nes Volcanic Field, *BBVF* Bakony–Balaton Upland Volcanic Field, *ST* Štiavnica basalts, *KE* Kecel basalts (buried), *LU* Lucaret basalt, *PVF* Perşani Volcanic Field



batch ascending rapidly from the mantle source, although recent studies revealed that composition of erupted magmas could change even within the eruptive sequence of a monogenetic volcano (Strong and Wolff 2003; Brenna et al. 2010; Erlund et al. 2010; McGee et al. 2012). Apart of these exceptions, basalts of monogenetic volcanoes provide a unique snapshot of the nature of the mantle source regions and could reveal their subtle compositional differences. Furthermore, basaltic products having composition close to the primitive magmas can be used to infer the condition of the mantle generation (pressure and temperature, mineral and chemical composition of the melted mantle

rock, degree of melting, mixing of melts, etc.). Using this knowledge, a better understanding can be achieved about the triggering mechanism of the melt generation and the geodynamic relationships of the volcanism. Nevertheless, recent studies have revealed that evolution of basaltic magmas could be far more complex than previously thought (Woodland and Jugo 2007; Smith et al. 2008; Jankovics et al. 2012, 2013) and careful investigation is necessary to select the most appropriate samples, which can be used to gain insight into the mantle and the melting process.

The Carpathian–Pannonian region (CPR; Fig. 1) is a key natural laboratory for studying the interaction of deep

mantle processes, igneous activity and tectonic events (Szabó et al. 1992; Seghedi et al. 1998, 2004a, b, 2005; Harangi 2001a; Konečný et al. 2002; Harangi and Lenkey 2007; Seghedi and Downes 2011). Alkaline basalt monogenetic volcanic fields have developed since 11 Ma, partly overlapping and partly postdating the extensive calc-alkaline andesitic–dacitic volcanism (Pécskay et al. 2006; Lexa et al. 2010). The alkaline basaltic volcanism is considered as part of the widespread Neogene to Quaternary volcanism in western and central Europe (Wilson and Downes 1991, 2006; Embey-Isztin and Dobosi 1995; Lustrino and Wilson 2007), but it shows many similarities also with the alkaline basaltic volcanism occurred with close spatial and temporal association of calc-alkaline and potassic–ultrapotassic volcanism in the Mediterranean (Wilson and Bianchini 1999; Harangi et al. 2006; Beccaluva et al. 2011). The origin of the basaltic volcanism in the CPR is still controversial (Embey-Isztin and Dobosi 1995; Embey-Isztin et al. 2001; Harangi 2001a, b; Seghedi et al. 2004a; Harangi and Lenkey 2007; Ali and Ntaflou 2011; Ali et al. 2013; Harangi et al. 2013), largely due to its occurrence after the main extensional phase of the Pannonian basin. Eruption of basaltic magmas took place even at a couple of 100's ka; thus, understanding the mechanism of melt generation is crucial also to evaluate rigorously whether this kind of volcanic activity could continue in the future.

In this paper, we discuss the conditions of the basaltic magma generation in the CPR using primarily those samples, which have chemical composition close to primitive magmas. We combine major and trace element data of the host basalts as well as compositional features of spinels, one of the liquidus minerals in these rocks, to constrain the origin of the magmas and the nature of the source regions. Then, we propose a possible mechanism that could be responsible for the formations of the basaltic volcanoes in this region.

## Geological setting

The CPR lies in the northeastern part of the Alpine–Mediterranean region and is characterized by an arcuate orogenic belt (Carpathians) with a basin area behind it (the Pannonian basin; Fig. 1a). The Pannonian basin is surrounded by the Alpine, Carpathian and Dinarides mountain belts. It is underlain by thin lithosphere (50–80 km) and crust (22–30 km) coupled with high heat flow ( $>80$  mW/m<sup>2</sup>; Csontos et al. 1992; Horváth 1993; Tari et al. 1999; Lenkey et al. 2002; Horváth et al. 2006). It is regarded as a special type of back-arc basin formed by heterogeneous stretching of the lithosphere. The thinning of the lithosphere started in the Early Miocene (around 20 Ma) and the syn-rift phase was finished by the end of Miocene (around

12 Ma; Horváth et al. 2006). Tari et al. (1999) defined an initial core-complex style extension during the Early Miocene followed by a wide-rift-type extension. Huisman et al. (2001) distinguished two main rifting events, involving a Middle Miocene passive rifting followed by a Late Miocene active rifting episode. As a consequence, the lithospheric mantle underwent a dramatic attenuation (stretching factor of 5–50), whereas the crust was only moderately thinned (stretching factor of 1.2–2.5) leading to the suggestion of an inhomogeneous stretching model (Sclater et al. 1980; Horváth et al. 1988, 2006). As an extreme case, Horváth et al. (2006) assumed the disappearance of the whole mantle lithosphere beneath the Pannonian basin at the beginning of the syn-rift phase. The thinning of the lithosphere was accompanied by asthenospheric mantle updoming as shallow as 50–60 km (Stegena et al. 1975; Huisman et al. 2001; Konečný et al. 2002), and therefore, the Pannonian basin can be considered as one of the hottest basin areas of Europe (Cloetingh et al. 2007). The syn-rift phase was followed by post-rift thermal subsidence, when several thousands meters of Late Miocene to Quaternary sediments filled parts of the basin areas (Great Hungarian Plain, Little Hungarian Plain).

There are diverse views on the driving mechanism of the lithospheric extension such as (a) formation of an overthickened hot lithosphere, which underwent gravitational collapse during the Early Miocene (Tari et al. 1999; Horváth et al. 2006); (b) suction of the slab rollback beneath the retreating subduction along the Eastern Carpathians (Csontos et al. 1992); (c) dripping the lower, gravitationally unstable lithospheric material into the deep mantle (Lorinczi and Houseman 2009) and (d) asthenospheric flow either via the “Istria window” beneath the Dinarides (Horváth and Faccenna 2011) or from the Adria–European collision zone and ensuing Alpine orogeny (Kovács et al. 2012). While the models (a) and (b) are supported by geophysical and geological observations and are widely accepted by the scientific community, the novel models (c) and (d) have still a number of inconsistencies and therefore need more supporting evidences.

Since the Pliocene, the CPR has been in a tectonic inversion stage (Horváth and Cloetingh 1996; Bada et al. 1999) due to the continuous push from west (Adria-push from the Alps–Dinarides belt) and blocking the area at east by the thick Ukrainian lithosphere. The entire basin system has been landlocked and this led to a gradual structural inversion in the form of multi-scale folding and fault reactivation. Some parts of the CPR (Great Hungarian Plain, Little Hungarian Plain and Danube basin, Vienna basin, Styrian basin and Brasov basin) are still subsiding, while other parts show uplift (Dombrádi et al. 2010). This differential vertical movement is accommodated by reactivation of older faults. Major strike-slip faults have a SW–NE orientation

at the northern and central part of the CPR, whereas to the south a characteristic E–W trending strike-slip fault system was identified (Horváth et al. 2006; Fig. 1b).

The nature of the upper mantle beneath the CPR is inferred from seismic tomographic models. These show a high-velocity body in the transition zone (400–670 km) interpreted as accumulated subducted slab material (Wortel and Spakman 2000; Piromallo and Morelli 2003; Hetényi et al. 2009), a near-vertical high-velocity slab beneath the southeastern margin of the CPR (Vrancea zone), regarded as the trace of final-stage subduction (Sperner et al. 2001, 2004) and relatively low-velocity material between the transition zone and the base of lithosphere.

### Areal distribution of the basalts

In the CPR, four main monogenetic volcanic fields were developed (Styrian, Bakony–Balaton Upland, Nógrád–Gemer, Perşani; Fig. 1b). In addition, localized basaltic centers were developed in a few areas (Pauliberg–Oberpullendorf in Burgenland, Lucaret–Sanovita in Banat), where no precursor and subsequent volcanism occurred. Basalt volcanic centers of the eastern part of the Little Hungarian Plain (called here Kemenes Volcanic Field, Fig. 1b) and around Štiavnica (ST in Fig. 1b) can be considered to form ultra-low-magma-flux volcanic fields, where volcanic activity was sporadic (<10 volcanic centers) during a considerable (2–6 Myr) timescale and characterized by several 100's ka (several Myr in ST) long quiescence time between the active events.

The basaltic volcanism was controlled by external conditions, such as tectonics, topography, presence and style of aquifer in the basement (Martin and Németh 2004; Kereszturi et al. 2011). Tuff rings and maar structures were developed as a result of phreatomagmatic explosive eruptions followed occasionally by pure magmatic explosive volcanism, and in a few cases, lava lakes were formed in the late-stage effusive phase. Large volcanic edifices, such as shield volcanoes, were built up in each volcanic field (Stradner Kogel in Styria, Kab, Agár and Fekete hills in the Bakony–Balaton Upland, Medvedia in Nógrád–Gemer) except for the Perşani. The volcanism was dominantly basaltic, the only exception is the Kemenes Volcanic Field, where a large trachyandesite–trachyte volcano developed around 10–11 Ma (Pásztori volcano; Harangi et al. 1995; Harangi 2001b). This volcano subsided subsequently and was covered by thick (over 2,000 m) Late Miocene to Quaternary sediments.

The geographic location of the volcanic fields in the CPR (Fig. 1b) is remarkable, since they are mostly at the western and northern margins of the Pannonian basin and not in the central area, where there is the thinnest

lithosphere, whereas the youngest one is found at the southeastern part of the region, close to the seismically active Vrancea zone. The two largest volcanic fields in the CPR are the Bakony–Balaton Upland Volcanic Field (Martin and Németh 2004) and the Nógrád–Gemer Volcanic Field (Konečný et al. 1995, 1999), each of them involves about 50 eruptive centers, have relatively long timescale of the volcanism (6–8 Ma), and includes intermittent active phases with relatively long (several 100's ka) repose time. Kereszturi et al. (2011, 2013) calculated the recurrence rate for both volcanic fields and got about 0.11 and 0.08 Ma/event, respectively. Although the volcanic edifices are deeply eroded in both areas, they estimated also the magma flux that is 0.9 km<sup>3</sup>/Ma (calculated only for the last five active phases, excluding the initial phase) and 0.4 km<sup>3</sup>/Ma, respectively (the total erupted magma volume is estimated to be about 4 and 3.5 km<sup>3</sup>, respectively). These numbers are comparable with the low-magma-flux monogenetic volcanic fields, such as the Southwestern Nevada Volcanic Field (Valentine and Perry 2007), and classify them as typical tectonically controlled, time predictive volcanic fields. The Styrian and Perşani Volcanic Fields (Seghedi and Szakács 1994; Downes et al. 1995; Ali et al. 2013; Harangi et al. 2013) contain less eruptive centers, although in Styria, the eruptive volume could be relatively large (>1 km<sup>3</sup> total volume) due to the significant amount of effusive volcanic products (Stradner Kogel, Klösch, Steinberg). The Perşani Volcanic Field is the youngest one in the CPR and is located in a 22-km-long and 8-km-wide area (Seghedi and Szakács 1994) at the northwestern periphery of the intramontane Braşov basin (Fig. 1b). This area is characterized by NE–SW trending normal faults, resulting from a NW–SE extensional regime (Gîrbacea et al. 1998). The eruptive centers appear to be structurally controlled and show a rough NE–SW trending alignment. Popa et al. (2012) recorded subcrustal seismicity beneath the Perşani area and, using seismic tomography modeling, suggested that a low-velocity anomaly could be inferred at the crust–mantle boundary. The youngest basalt volcano (Putikov vršok; Šimon and Halouzka 1996) of the CPR is located near Banská Štiavnica upon the Late Pleistocene terrace of the river Hron. It does not rigorously belong to the Nógrád–Gemer Volcanic Field and was formed after more than 6 Ma quiescence in this area. There are two “satellite volcanoes” in the CPR: The alkaline basalts of Pauliberg and Oberpullendorf are found at the Alps–Pannonian Basin transition zone in Burgenland (Harangi 2001b; Ali and Ntaflou 2011) and represent a single volcanic episode at about 11 Ma. Harangi et al. (1995) suggested that they could have some compositional similarities with the basaltic dyke rocks in the Pásztori volcano. In the southern part of the CPR, the

alkaline basalt of the Lucaret–Sanovita belongs also to a single eruptive event without any precursor magmatism. It is located close to a major west–east trending strike-slip zone (Fig. 1b) and at the boundary of subsiding and uplifting areas (Dombrádi et al. 2010). Remarkably, further single—potassic—ultrapotassic—volcanoes (Bár, Uroi) were formed also along this tectonic line during the last 2.5 Ma.

### Temporal evolution

Monogenetic basalt volcanic fields are typically active over millions of years. The volcanism is characterized by intermittent eruptions gathering often in active phases, which are separated by long repose periods. Recurrence rate of volcanism is particularly important in evaluating the volcanic hazard (Condit and Connor 1996; Valentine and Perry 2007), although precise dating of eruptions is difficult for basaltic rocks. In the Pannonian Basin, eruption ages were determined mostly by K/Ar radiometric technique (Balogh et al. 1982, 1986, 1990, 1994; Borsy et al. 1986). Ar/Ar dating was performed for the basaltic rocks of the Bakony–Balaton Upland volcanic fields that corroborated the reliability of the former K/Ar data (Wijbrans et al. 2007). In contrast, the new Ar/Ar age data (Panaiotu et al. 2013) refined significantly the former knowledge (Panaiotu et al. 2004) on the temporal evolution of the Perşani volcanic field. So far, the available K/Ar database provides a solid framework for the temporal evolution of the alkaline basaltic volcanism in the Pannonian basin, although more careful studies are necessary to define the recurrence rates in individual volcanic fields more precisely and constrain the eruption age of the youngest volcanic episodes.

In the Pannonian Basin, eruption of alkali basaltic magmas started in the westernmost margin, where two outcrops are known, at Pauliberg and at Oberpullendorf in Burgenland (Ali and Ntaflou 2011), and their ages were determined as 11.7–10.5 Ma (Balogh et al. 1994). Similar ages were published for the basalts found in drilling cores around Kecel (central Pannonian basin; 8.1–10.4 Ma; Balázs and Nusszer 1987). Although these basalts are strongly altered, their Late Miocene ages were corroborated by stratigraphic data.

The basaltic volcanism in the two largest volcanic fields (Bakony–Balaton Upland and Nógrád–Gemer) lasted for more than 6 Myr. Noteworthy, eruption of basaltic magmas in both areas commenced at 7.8–8.0 Ma (Balogh and Németh 2005; Balogh et al. 2005; Chernyshev et al. 2013) and continued after 2 Ma quiescence in the Bakony–Balaton Upland and after about 1 Ma repose time in the Nógrád–Gemer area. The volcanism in both areas was characterized by closely packed active phases separated by long repose

periods (Konečný et al. 1995, 1999; Wijbrans et al. 2007). Kereszturi et al. (2013) estimated the peak magma output times being at 3–4 Ma in the Bakony–Balaton Upland volcanic field and 1.5–3.0 Ma in the Nógrád–Gemer area. The alkaline basalt occurrences cropping out within the area of the Middle Miocene eroded andesitic Štiavnica composite volcanic complex are spatially separated from the Nógrád–Gemer volcanic field. They show highly sporadic eruption times, such as 6.6–7.8 Ma in Banská Štiavnica and Dobrá Niva and 0.1–0.5 Ma for the Putikov volcano at the Hron river (Balogh et al. 1981; Konečný et al. 1999; Šimon and Halouzka 1996; Šimon and Maglay 2005; Chernyshev et al. 2013). The age of the Putikov vršok volcano has a particular importance, since it indicates the latest alkaline basalt eruption in the CPR. Balogh et al. (1981) and later Chernyshev et al. (2013) provided 430–530 ka eruption ages using K/Ar technique, whereas Šimon and Halouzka (1996) considered the stratigraphic position of the lava flow and interpreted it as sitting on the Late Pleistocene (Riss) terrace of the Hron river, and this points to an age of 120–150 ka. This younger age was supported by optically stimulated luminescence (OSL) dating of the underlying sediments that yielded an age of  $102 \pm 11$  ka. Further investigation is necessary and highly important to constrain the exact eruption age of this basalt. The youngest eruption ages in the Nógrád–Gemer volcanic field require also detailed investigation. In the last intense eruptive phase between 1.1 and 1.5 Ma, mostly effusive activity was recognized (Konečný et al. 1995, 1999). The latest eruptions in this area was previously thought to have occurred around 400 ka (Hodejov and Fil'akovo maars; Konečný et al. 1995); however, new (U–Th)/He zircon dating (Hurai et al. 2013) did not confirm this young age.

In the western margin of the CPR (Styrian basin; Ali et al. 2013), alkaline basaltic volcanism occurred between 3.9 and 1.9 Ma (Balogh et al. 1994) after a long quiescence period since the 14.0–17.5 Ma high-K trachyandesitic volcanic activity (Harangi et al. 1995). The latest eruption resulted in a relatively large volume shield volcano composed of nephelinites at Stradner Kogel.

The youngest monogenetic volcanic field of the CPR is located at the western margin of the Perşani Mts., between the Transylvanian basin and the Brasov basin (Seghedi and Szakács 1994; Downes et al. 1995; Harangi et al. 2013). Although former K/Ar and paleomagnetic dating (Panaiotu et al. 2004) implied two, well-separated eruption phases, the new Ar/Ar dating (Panaiotu et al. 2013) revised this and indicated a fairly continuous, but very scattered volcanism from 1.22 to 0.52 Ma.

Finally, a unique basalt occurrence is found at Lucaret (southern Pannonian basin), where no precursor volcanic activity took place and the age of this basalt was determined as 2.4 Ma (Downes et al. 1995).

## Petrologic and geochemical characteristics

Petrologic and geochemical features of the alkaline basaltic rocks of the CPR have been published in several papers (Embey-Isztin et al. 1993, 2001; Seghedi and Szakács 1994; Dobosi et al. 1995; Downes et al. 1995; Harangi et al. 1995, 2013; Harangi 2001b; Harangi and Lenkey 2007; Ali and Ntaflou 2011; Tschegg et al. 2010; Jankovics et al. 2012, 2013; Ali et al. 2013), and we completed them with new analysis, mostly from the Nógrád–Gemer Volcanic Field (Sági and Harangi 2013). Representative composition of the basalts from different locations is given in Table 1. In this section, we provide a brief summary on the main features of the basalts.

The basaltic rocks are classified as alkali basalts, trachybasalts, basanite, phonotephrite and nephelinite (Fig. 2). Evolved rocks types occur in the buried Pásztori volcano, and they are trachyandesite and trachyte (Harangi et al. 1995; Harangi 2001b). Most of the basalts are olivine-phyric, while clinopyroxene phenocryst is found in a few localities of the Bakony–Balaton Upland and Kemeses Volcanic Field, but is more common in the basalts of the Styrian Volcanic Field and in the Nógrád–Gemer Volcanic Field. The olivine phenocrysts with Fo >84 mol % often contain spinel inclusions, and these two minerals can be regarded as liquidus phases. Both minerals have a wide compositional range (Ali and Ntaflou 2011; Jankovics et al. 2012, 2013; Ali et al. 2013; Harangi et al. 2013). The most magnesian olivines have typically high Mn content compared with the trend defined by Herzberg (2011) for olivines crystallized from peridotite-derived magmas. They are characterized by low Fe/Mn ratio (Fe/Mn = 40–75); this feature along with the relatively low Ni content (<2,500 ppm) is not consistent with derivation of the primary magmas from pyroxenite source as defined by Sobolev et al. (2007) and Herzberg (2011). Clinopyroxene phenocrysts could have crystallized mostly at the crust-mantle boundary zone as shown by the geobarometric calculations. Their complex zoning often found in basalts from the Nógrád–Gemer and the Bakony–Balaton Upland indicates mixing of magma batches at depth (Dobosi 1989; Dobosi and Fodor 1992). Mantle-derived ultramafic and lower crustal granulite xenoliths are common in basalts of each volcanic field (Embey-Isztin et al. 2001; Szabó et al. 2004).

The CPR basalts are almost exclusively silica-undersaturated and have Mg-numbers ranging from 0.5 to 0.8 (MgO = 5–15 wt%). The most magnesian basalts contain, however, significant amount of xenocrysts (e.g., Bondoró and Füzes at Bakony–Balaton Upland), which strongly modify the bulk rock composition (Jankovics et al. 2012, 2013). Majority of the basalts have an Mg-number >0.62, suggesting only a minor to moderate

effect of fractional crystallization. Moderately fractionated basalts are found mostly in Styria and in the Nógrád–Gemer areas. For this study, we selected those samples that have Mg-number between 0.64 and 0.72 (MgO = 8–13 wt%), and therefore, their compositions are close to that of the primitive magmas. In these samples, variation of major elements indicates the controlling factor of various amounts of olivine fractionation. However, characteristic differences can be recognized between the most primitive basalts. The Pauliberg basanite has a distinct composition with low Al<sub>2</sub>O<sub>3</sub> and high TiO<sub>2</sub> and FeO contents (Fig. 3). Experimental studies suggest that such composition could be obtained by low-degree melting of carbonated, silica-deficient eclogite (Dasgupta et al. 2006; Kogiso and Hirschmann 2006). The basalts from Oberpullendorf (Burgenland) and Putikov vršok (Štiavnica) have a transitional major element composition between the Pauliberg basanite and the rest of the CPR basalts.

The trace element composition of basalts resembles those commonly found in intraplate magmas and is similar to the Neogene to Quaternary alkaline mafic rocks in western and central Europe (Wilson and Downes 1991; Lustrino and Wilson 2007). The FTS elements, such as Ni, Cr and Sc, have relatively high abundances (Ni = 100–300 ppm; Cr = 100–500 ppm; Sc = 10–30 ppm; Fig. 3) consistent with the slight olivine ± spinel-dominated fractional crystallization. Based on the primitive mantle (McDonough and Sun 1995) normalized trace element patterns, Harangi and Lenkey (2007) defined two main compositional groups: The first one is characterized by stronger enrichment in incompatible trace elements and a typical negative potassium anomaly, whereas the second one has smoother trace element patterns and no negative potassium anomaly (Fig. 4). The strongly incompatible trace elements have a wide compositional range (La = 25–90 ppm, Nb = 30–130 ppm, Th = 3–13 ppm; Fig. 3) and show a positive correlation with an intercept of zero. Same covariance with Ba can be also observed although the basalts from Pauliberg and Styria show a distinct trend.

Sr–Nd–Pb isotope ratios of the basalts were published by Embey-Isztin et al. (1993), Dobosi et al. (1995), Downes et al. (1995) and Harangi et al. (1995). All of the basalts fall into the depleted field in Sr–Nd isotope space, similar to majority of the Neogene to Quaternary alkaline mafic rocks in western and central Europe (Wilson and Downes 1991; Wilson and Patterson 2001). The most depleted end member of this variation trend is a mixture of HIMU and DMM. In the Pb–Pb isotopic diagrams, they show a relatively large variation, many of the samples have relatively high <sup>207</sup>Pb/<sup>204</sup>Pb ratio (>15.6) causing a vertical shift from the NHRL. The highest <sup>206</sup>Pb/<sup>204</sup>Pb ratio (19.6–19.7) is shown by the Pauliberg basanite.

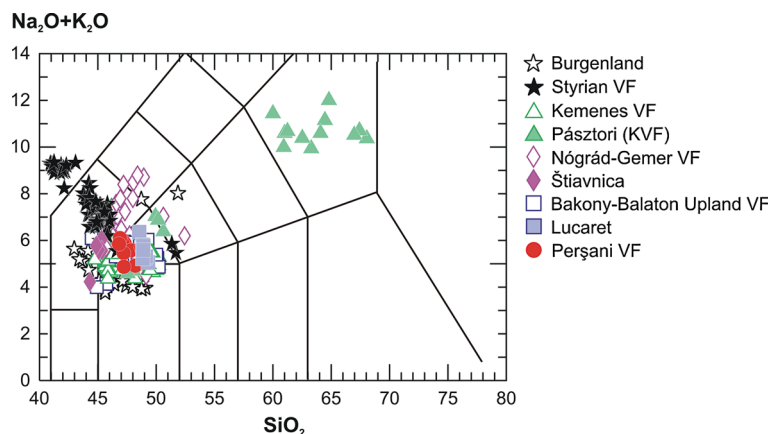
**Table 1** Representative major and trace element composition of the basalts from different volcanic fields of the CPR

Sample	KL-4	ST-11	PLB-4	OB-1	SAG08-2	S-1	KK-1	PUT-2	CSAM1	LU52	BARC
Locality	Klöch	Steinberg	Pauliberg	Oberpul-lendorf	Ság	Sátorma	Kapolcs	Putikov	Belinsky vrch	Lucaret	Barc
Volcanic field	SVF	SVF	BU	BU	KVF	BBVF	BBVF	SE	NGVF	LU	PVF
Reference	1	1	2	2	3	3	3	3	3	3	4
SiO <sub>2</sub>	44.97	43.87	46.99	49.07	48.19	47.24	46.53	44.32	48.43	48.90	46.82
TiO <sub>2</sub>	2.25	2.12	3.76	2.73	2.31	2.18	2.24	2.53	1.94	2.23	1.78
Al <sub>2</sub> O <sub>3</sub>	15.58	14.92	11.13	12.75	14.10	15.51	15.37	13.64	15.07	14.45	16.01
Fe <sub>2</sub> O <sub>3</sub>	10.03	11.02	12.59	11.58	11.79	10.35	10.86	12.11	10.91	10.82	10.16
MnO	0.17	0.20	0.15	0.20	0.14	0.16	0.15	0.19	0.16	0.15	0.17
MgO	9.40	8.19	10.54	9.14	9.55	9.03	9.61	11.32	10.03	8.54	9.26
CaO	10.19	10.80	9.95	10.13	9.04	8.80	9.26	10.62	7.82	8.58	9.48
Na <sub>2</sub> O	4.58	5.47	2.78	2.65	2.83	3.65	3.13	2.91	3.86	4.00	3.93
K <sub>2</sub> O	2.11	2.37	1.48	1.31	1.53	2.30	2.18	1.32	1.45	1.76	1.92
P <sub>2</sub> O <sub>5</sub>	0.72	1.06	0.62	0.44	0.50	0.79	0.67	1.04	0.32	0.57	0.48
LOI	0.98	0.23	0.11	2.12	2.1	1.6	1.4	2.4	0.2	-0.4	-0.1
Mg-number	0.69	0.63	0.66	0.65	0.65	0.67	0.67	0.69	0.68	0.65	0.68
SI	-27.25	-38.32	-3.19	2.40	-0.44	-12.19	-10.31	-11.85	-6.60	-8.17	-16.11
Ni	138	123	274	324	228	200	172	238	234	138	179
Cr	136	121	332	287	356	246	260	383	191.5766	177	315
V	215	206	172	200	198	182	176	216	180	144	194
Sc	19.4	13.6	16.4	20.9	21	19	22	24	19	10.1	26
Co	38.1	36	51.5	45.6	48.7	41.4	41.4	47.8	51.2	41.4	41.1
Rb	52.8	62.2	39.8	21.2	26.5	56.8	50.7	27.8	32	36	43.1
Ba	581	713	479	305	602	877	627	617	445	464	758
Sr	1,008	1,203	881	577	808.1	1,159.2	1,385.8	1,011	684.5	627	775
Zr	368	556	498	364	187.8	282.9	194.7	262.9	152	183	185.3
Nb	94.2	111	72.4	49.8	40.9	80.1	53.3	82.6	38.5	51.4	51.8
Y	28.5	34.3	31.4	27.3	21.1	27.5	21.5	23.8	19.4	22.6	23.8
Th	9.9	12.6	5.26	3.64	4.7	8.8	6.7	6.2	3.3	4.72	6
La	56.6	75.4	43.4	25.9	29.8	52.9	36.2	48.1	25.8	29.5	32.8
Ce	104	135	94.8	64.2	59.8	101.3	72.1	93.4	48.9	60	63.9
Pr	11.4	14.5	12.1	6.9	7.81	12.2	9.11	11.35	5.57	7.61	7.59
Nd	46.2	59	49.7	30.7	31.6	48.7	37.8	46.9	22.5	31.5	34
Sm	7.26	8.97	10.5	6.16	6.87	8.13	6.69	8.65	4.6	7.12	6.04
Eu	2.24	2.71	3.07	1.92	2.13	2.36	2.05	2.49	1.48	2.23	1.86
Gd	6.68	8.09	9.2	5.82	5.86	6.76	5.67	6.86	4.42	6.28	5.14
Tb	0.87	1.02	1.23	0.806	0.85	0.8	0.73	0.83	0.71	0.94	0.7
Dy	4.45	5.15	5.89	4.11	4.37	4.86	4.22	4.91	3.92	4.92	4.35
Ho	0.82	0.94	1.04	0.755	0.74	0.84	0.78	0.8	0.7	0.94	0.83
Er	2.1	2.43	2.53	1.87	1.87	2.21	1.95	1.99	1.91	2.38	2.26
Tm	0.28	0.32	0.312	0.249	0.28	0.31	0.28	0.27	0.27	0.31	0.34
Yb	1.8	2.04	1.91	1.53	1.49	1.88	1.52	1.6	1.65	2	2.21
Lu	0.25	0.28	0.246	0.21	0.21	0.28	0.24	0.22	0.24	0.28	0.31
Hf	5.96	8.82	9.32	6.16	4.9	6	4.8	5.6	3.6		4.5
Ta	5.12	6.82	3.43	2.69	2.1	4.5	3.3	4.8	2.4	2.85	3.1
U	2.54	3.03	1.57	0.917	0.9	2.3	1.8	2	0.8	1.35	1.7
$p_f$	2.8		3.1	2.5	2.35	2.2	2.2	3.35	2.55	2.75	2.15
$p_o$	2.9		3.8	3.8	3	2.8	2.9	3.6	3	3.2	2.6
$T$	1,390		1,472	1,416	1,376	1,343		1,418	1,386	1,395	1,378
$p$	2.72		2.61	1.86	2.05	2.10		2.91	2.00	1.99	2.21

$p_f$  and  $p_o$  are the calculated final and initial melting pressures, respectively, using the Langmuir et al.'s (1992) model.  $T$  and  $p$  are the mantle potential temperature and the melting pressure using the thermobarometer of Lee et al. (2009) with molar  $Fe^{3+}/Fe^{tot} = 0.13$

Reference: 1: Ali et al. (2013), 2: Ali and Ntaflou (2011), 3: this study, 4: Harangi et al. (2013)

**Fig. 2** Classification of the basalts based on the TAS diagram (Le Bas et al. 1986). The used data set is found in the supplementary table along with the references to the sources of the data. Data of the Pásztori trachyte are from Harangi et al. (1995) and Harangi (2001b)



## Discussion

Most of the alkaline basalts of the CPR show chemical composition ( $\text{MgO} > 8 \text{ wt\%}$ ;  $\text{Ni} = 130\text{--}350 \text{ ppm}$ ; Fig. 3) that could be close to that of the primitive magmas. Using only these samples, the condition of the melting process as well as the nature of the source region can be constrained that could contribute to our understanding on the reason of mantle melting beneath the area. Trace element ratios such as  $\text{Nb/Th}$  (5–15) and  $\text{Nb/La}$  (1–2) of the basalts show values that are higher than those observed in continental crustal rocks (Rudnick and Fountain 1995) and are typical of mantle-derived melts, mostly for those derived from the asthenosphere. Therefore, we can conclude that crustal contamination did not significantly modify the trace element composition of the CPR mafic magmas. Most of the selected basalts are olivine-phyric, and the olivine phenocrysts often contain spinel inclusions, indicating that these mineral phases could have been liquidus minerals as have been suggested for the usual evolution of alkaline silica-undersaturated mafic magmas (Roeder et al. 2006). High-pressure clinopyroxene crystallization could modify the magma composition as well as the composition of coexisting evolving phases, and this should be considered even in the absence of clinopyroxene phenocrysts in the rocks (Smith et al. 2008). This would decrease the  $\text{CaO}$  content of the magma and possibly also leads to lowering the  $\text{CaO}$  content of the olivine phenocrysts. Nevertheless, our geothermobarometric calculations on selected clinopyroxenes in some basalts (Harangi et al. 2013) suggest that they crystallized later than the olivines. The relatively high  $\text{Sc}$  content of the basalts ( $\text{Sc} > 15 \text{ ppm}$  except for the samples from Lucaret) and the uniform  $\text{Cr}$ -number of the spinels along with various  $\text{Fo}$  content of coexisting olivines also imply that no significant early-stage clinopyroxene fractionation occurred that would significantly modify the magma composition. Taking all of this into account, the composition of the alkaline basalts with  $\text{Mg} > 8 \text{ wt\%}$  can

be used to infer the melting condition and the nature of the source rock.

In this discussion, we attempt to constrain the origin of the magmas using the following principle: We consider the simplest model over the complex models and take a complex model only when no simple model works (Niu 2005). Thus, we simplified the mantle source material considering to be dominantly peridotitic in lithology, knowing, however, that involvement of more fusible material, such as pyroxenite or eclogite, could be possible. There are some inferences for the existence of such material in the mantle source region, but we think that further careful investigation is necessary to test their influence on the melting models and the composition of the primary magmas.

### Asthenospheric versus lithospheric mantle source region

Origin of the continental intraplate basaltic rocks is often debated. Alkaline silica-undersaturated mafic magmas are considered being generated by low degree of melting either in the upwelling asthenosphere (Bradshaw et al. 1993; Wang et al. 2002; Niu et al. 2011; Gazel et al. 2012) or by melting of metasomatic, usually amphibole-rich veins in the lithosphere (Fitton et al. 1991; Ormerod et al. 1991; DePaolo and Daley 2000; Beccaluva et al. 2007; Valentine and Perry 2007; Bianchini et al. 2008; Pilet et al. 2008; Mayer et al. 2013, 2014). Variation of trace element and isotopic compositions of the Neogene to Quaternary basaltic rocks in Europe led Wilson and Downes (1991, 2006) to conclude that both mantle regions could have contributed to the magma generation. This was reinforced by the more specific studies in various parts of volcanic areas in Europe (Haase et al. 2004; Haase and Renno 2008; Jung et al. 2012), including the Pannonian basin (Embey-Isztin and Dobosi 1995; Harangi 2001a; Seghedi et al. 2004a, b) and was suggested also for the origin of the basaltic magmas in the western USA (Fitton et al. 1988, 1991), in the Auckland volcanic field, New Zealand (McGee et al.

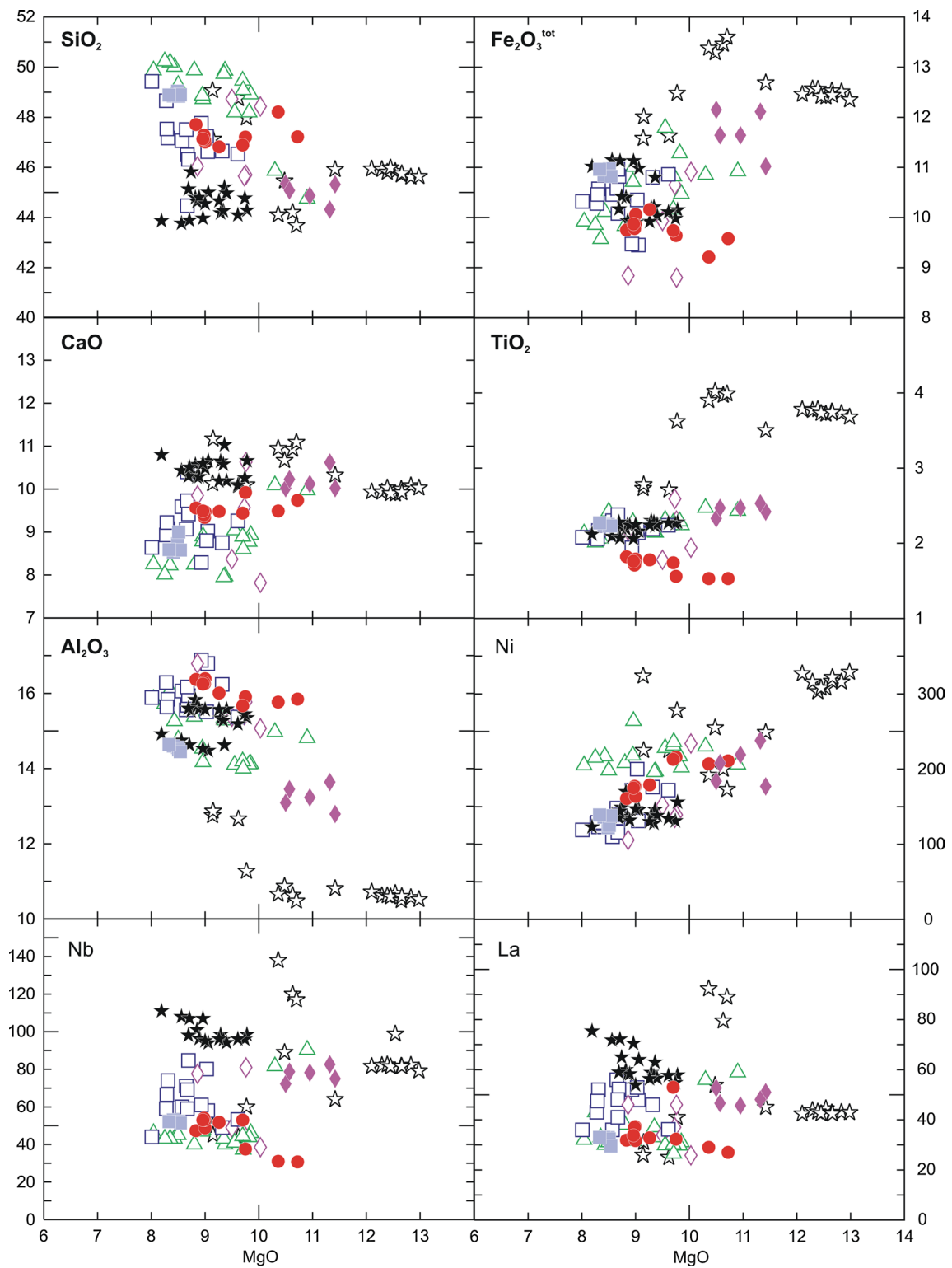


**Fig. 3** Selected major elements (in wt%) and trace elements (in ppm) versus MgO for the CPR basalts. *Symbols* as in Fig. 2

2013) and western Syria (Ma et al. 2011). However, an important question is why the colder lithospheric mantle undergoes melting. For this, the presence of fusible

material (metasomatic veins) and either significant thinning of the lithosphere or a thermal perturbation (heating) are necessary. The fusible material is usually considered to

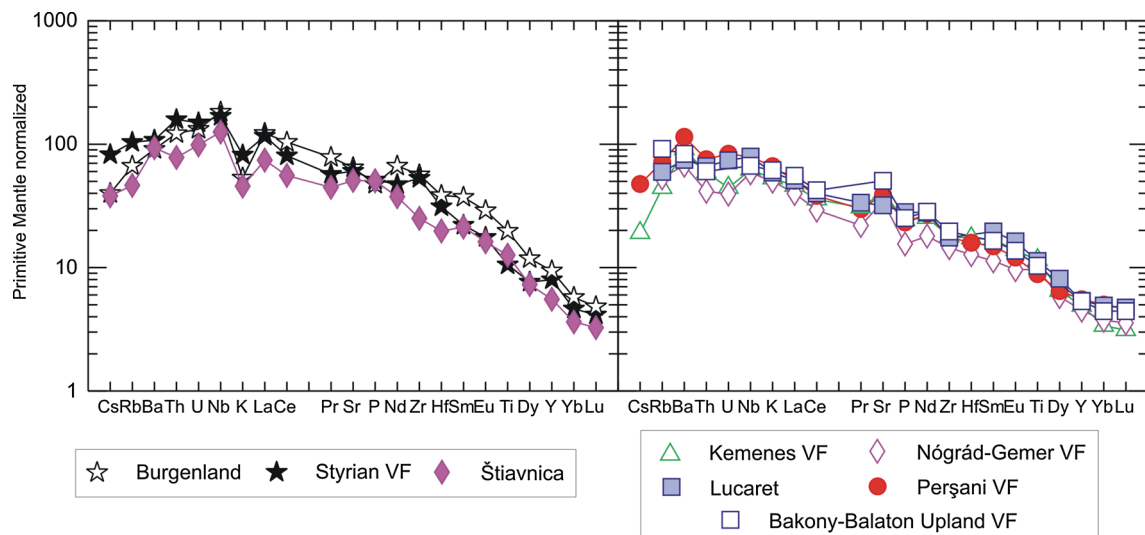


**Fig. 4** Primitive mantle (McDonough and Sun 1995) normalized trace element patterns for representative CPR basalts. Note that two groups can be distinguished based on the incompatible trace element abundances and the existence of negative K-anomaly

be amphibole-bearing veins, which originated from low-volume asthenospheric melts and are frozen in the lower lithosphere (McKenzie 1989; Niu 2008; Pilet et al. 2008; Humphreys and Niu 2009). The presence of amphibole in the source region is usually inferred based on the negative K-anomaly in the primitive mantle normalized trace element patterns (Class and Goldstein 1997; Späth et al. 2001; Jung et al. 2005; Haase and Renno 2008). Amphibole is stable up to about 1,100 °C temperature and up to about 2.5–3.0 GPa (ca. 100 km depth) and is regarded to be confined to the lithospheric mantle (Wallace and Green 1991).

The negative K-anomaly as expressed by the  $K/K^*$  ratio (calculated as  $K_N/\sqrt{(Nb_N * La_N)}$ , where  $K_N$ ,  $Nb_N$  and  $La_N$  are primitive mantle normalized values) is a characteristic feature of many of the CPR basalts and shows a wide continuous range ( $K/K^* = 0.3\text{--}1.2$ ; Fig. 5). It has a negative correlation with the  $La/Y$  and  $(Sm/Yb)_N$  ratios, which are the indicators of the degree and the relative depth of melting. This could suggest that a K-bearing phase, presumably amphibole, was present in the source of all of the CPR magmas and remained in the residual mantle during low-degree melting and entered into the melt in the case of larger melting. In that situation, the source of the magmas should be entirely the lithospheric mantle. Melting of the lower lithosphere in the post-rift phase of the Pannonian basin cannot be explained by decompression-driven process, but only by thermal perturbation, i.e., via heat flux from the underlying asthenospheric mantle. Taking this view, Seghedi et al. (2004b) postulated localized mantle plumes (plume fingers) beneath the basalt volcanic fields of the CPR. However, there is lack of physical evidences for the generation of localized hot mantle upwelling scattered beneath the CPR, and there is a lack of explanation

why this does not occur beneath the central Pannonian basin, where there is the thinnest lithosphere. Furthermore, the lowest  $K/K^*$  value is shown by the basalts having the highest  $(Sm/Yb)_N$  ratios and therefore reflects garnet in the source region. This would mean melting at depth  $>80$  km, which is already the asthenospheric mantle beneath most part of the region. Nevertheless, theoretically, it is possible that the high  $(Sm/Yb)_N$  ratio is inherited in the metasomatic vein (Pilet et al. 2008). Although Pilet et al. (2008) claimed that preferential melting of this material would yield magma composition akin to alkaline mafic magmas, others suggest that in this case potassic magmas are generated (McKenzie 1989; Wilson and Downes 1991; Cebriá and López-Ruiz 1995). Furthermore, the  $K/K^*$  ratio in the CPR basalts has no correlation with the  $La/Nb$  ratio that is used as an indicator of the lithospheric mantle (Fitton et al. 1991). In addition, the  $La/Nb$  ratio of the CPR basalts is  $<1$ , which is characteristic of asthenosphere-derived magmas. Finally, many alkaline OIB, such as St. Helena-type basalts (Chaffey et al. 1989; Kawabata et al. 2011), show negative K-anomalies, typically those formed by low-degree melting. Although melting of metasomatized lithosphere cannot be excluded as a potential origin of such basalts (Pilet et al. 2005, 2008), most authors consider them as derived from upwelling hot mantle beneath the oceanic lithosphere. Thus, this compositional feature could be rather general both in oceanic and continental realms and could be an inheritance in the mantle source regions, possibly representing the most fusible part (eclogite or pyroxenite with negative K-anomaly and HIMU/FOZO characteristics; Sobolev et al. 2005, 2007; Fekiacova et al. 2007; Dasgupta et al. 2010; Timm et al. 2009) of the melted mantle material. In this context, it is noteworthy that a correlation

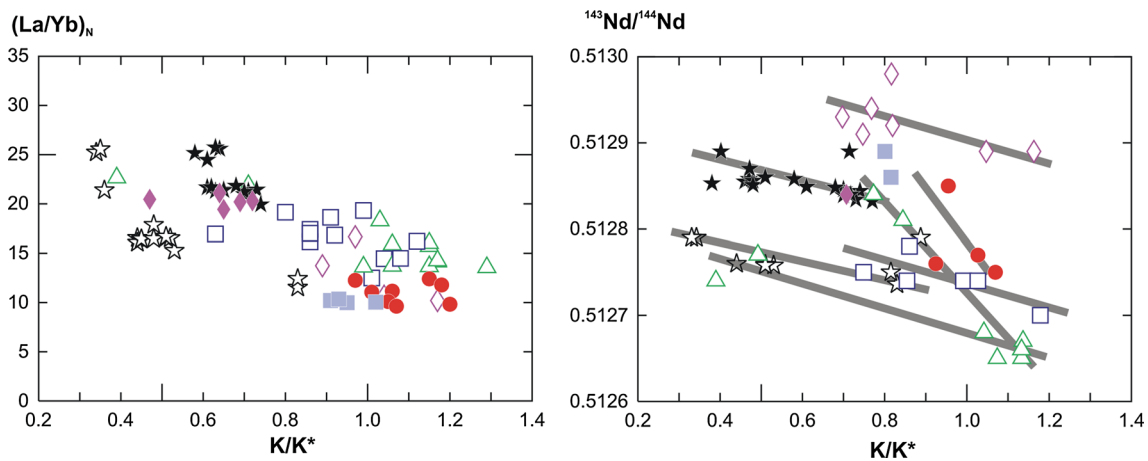


**Fig. 5**  $(La/Yb)_N$  versus  $K/K^*$  and  $^{143}Nd/^{144}Nd$  versus  $K/K^*$  diagrams for the CPR basalts. Note the negative correlation between these variables suggesting formation of the strongest negative K-anomaly in the melts generated at small degree of melting where garnet remained in the residue. The covariance between  $^{143}Nd/^{144}Nd$  and  $K/K^*$  in the

different basalt volcanic fields of the CPR implies that the negative K-anomaly could be inherited in the mantle source regions. The  $K/K^*$  is calculated as  $K_N/\sqrt{(Nb_N \cdot La_N)}$ , where N denotes normalization to the primitive mantle (McDonough and Sun 1995) values. Symbols as in Fig. 2

between the  $K/K^*$  value and the radiogenic isotope ratios ( $^{87}Sr/^{86}Sr$  and  $^{143}Nd/^{144}Nd$ ; Fig. 5) is observed within the volcanic fields and that can be more readily explained by derivation of the magmas with compositionally distinct mantle sources. Lower degrees of melting would produce magmas from the more fusible parts of the source region that are characterized by low  $^{87}Sr/^{86}Sr$  and high  $^{143}Nd/^{144}Nd$  isotope ratios similar to HIMU/FOZO (Stracke et al. 2005) and negative K-anomaly (low  $K/K^*$ ), whereas higher degree of melting would lead to mixing with melts coming from compositionally distinct mantle domains (Harangi and Lenkey 2007).

In summary, derivation of the basaltic magmas solely from the lithospheric mantle does not seem to be a plausible model in the CPR. In turn, we suggest that composition of the CPR basalts is consistent with melting predominantly or even entirely of the asthenospheric mantle. Since there are no convincing evidences for the existence of mantle plume or plume fingers beneath this region, nor progressive lithospheric extension, we think that it is physically difficult to generate significant amount of alkaline sodic magmas in the lithosphere during the post-rift and tectonic inversion stages unless considering local detachment and sinking of lithospheric fragments into the asthenosphere (Timm et al. 2010). At this stage, we think that composition of the CPR basaltic rocks reflects mostly the nature of the source region of the asthenospheric mantle and the heterogeneity within it.

#### Constraints on melting columns

Considering that the basaltic magmas in the CPR could derive predominantly from the asthenospheric mantle, an

upward mantle flow is required to initiate melting. As the solid mantle material moves upward adiabatically, melting starts when the ambient temperature intersects the solidus (initial melting pressure; Langmuir et al. 1992). This depth depends on the mantle potential temperature as well as the nature of the mantle material (Langmuir and Forsyth 2007), but for alkaline mafic magmas it is usually within the garnet stability field, i.e., deeper than 80 km (Niu et al. 2011). Melt production continues during further upwelling, and as a result, the initial magma composition will change due to the increasing extent of melting and according to the changing mineral assemblage of the melted mantle rocks (from garnet to spinel). Thus, the early-stage melt shows strong garnet-signature (high Ce/Y, Nb/Y and  $[Sm/Yb]_N$  ratios; Ellam 1992; Salters and Hart 1989; Putirka 1999; Niu et al. 2011), but it becomes progressively diluted in the strongly incompatible elements and loses their garnet fingerprint. The extent of the melting column (defined by the initial and final melting pressures, denoted as  $p_0$  and  $p_f$ , respectively) depends primarily on the thickness of the lithosphere (Ellam 1992; Langmuir et al. 1992; Putirka 1999; Niu et al. 2011). Melting beneath thick lithosphere stops at greater depth and therefore produces smaller amount of magma, which are enriched in strongly incompatible trace elements and have a pronounced garnet-signature, whereas in areas where the lithosphere is thinner, melting could continue even in the spinel-stability field and produces more melt with different incompatible element abundances. Thus, the  $p_f$  can be used as a proxy for the thickness of the lithosphere, i.e., defining the depth of the lithosphere–asthenosphere boundary (LAB).

The pressure of the melting can be constrained by various methods. Major element composition of the primitive magmas is influenced by the pressure of melting and the extent of melting (Takahashi and Kushiro 1983; Langmuir et al. 1992; Hirose and Kushiro 1993; Baker and Stolper 1994; Walter 1998; Niu et al. 2011). MgO and  $\text{FeO}^{\text{t}}$  increase and  $\text{SiO}_2$  decreases with increasing pressure of melting, whereas the  $\text{Na}_2\text{O}$  content of the primary magma depends mostly on the degree of melting. The CPR basalts have a relatively wide range of FeO content ( $\text{FeO}^{\text{t}} = 8\text{--}12$  wt%; Fig. 3) showing an inverse correlation with  $\text{SiO}_2$ , indicating that the primary magmas could have formed at various pressures. In order to quantify the pressure of melting, i.e., the depth of the magma generation first, correction of fractional crystallization has to be performed. This can be achieved by adding as much olivine to the bulk rock composition until the Mg-number is around 0.72, consistent with a primitive melt composition that is in equilibrium with a melted peridotite with olivine having Fo content around 0.9 mol%. For the selected mafic rocks of the CPR, correction of 5–15 % olivine fractionation was necessary.

Langmuir et al. (1992) developed a model where the  $\text{FeO}^{\text{t}}$  and  $\text{Na}_2\text{O}$  contents of the primary magmas are used to constrain the initial and final pressure of melting. Although this was constructed for mid-ocean ridge basalts, Wang et al. (2002) demonstrated that it provides reliable results for most melting within the depth interval of 50 and 110 km. The melting model lines were compared with experimentally determined peridotite melts, and a good reproduction was obtained between 1.0 and 4.0 GPa. Furthermore, Wang et al. (2002) emphasized that for magmas having  $\text{Na}_2\text{O} > 3$  wt% that is relevant for the CPR basalts, the model is not dependant upon the melt pooling mechanism. We used this model calculation, considering accumulated fractional melting process to determine the melting columns under the alkaline basalt volcanic field of the CPR. In the Fig. 6a, each curve represents a different initial melting pressure, i.e., where the ambient mantle temperature intersects the solidus. The total iron content of the magma reflects the condition of the onset of melting, i.e., the initial pressure that has a close relationship also with the mantle temperature. As melting proceeds, the volume of magma increases and as a consequence the concentration of incompatible elements as well as  $\text{Na}_2\text{O}$  decreases, while the total iron concentration does not change significantly. Therefore, the final values of the  $\text{FeO}^{\text{t}}$  and the  $\text{Na}_2\text{O}$  of the accumulated melt yield information on the initial melting pressure and the cessation of the melting, i.e., the final melting pressure. These pressure values are then converted to depth, assuming average densities of crust and mantle, 2.85 and 3.25  $\text{g/cm}^3$ , respectively, as suggested by Wang et al. (2002). The crustal thickness was taken as 32 km

beneath Burgenland (western CPR) and 35 km beneath Perşani (eastern CPR), whereas 28 km was used for the rest of the areas. Note that the pressure/depth estimate has an about 10–20 km uncertainty due to various effects such as the estimate of the primary composition, mantle fertility and the neglecting  $\text{Fe}^{3+}$  in the iron content of the primitive melts (Wang et al. 2002).

We obtained  $p_0$  and  $p_f$  values for 13 basalt localities that cover all the monogenetic volcanic fields of the CPR (Fig. 6a). Within them, only one basalt group from the Nógrád–Gemer Volcanic Field shows a melting column with a depth interval that seems to be unusually shallow (2.0–1.55 GPa, i.e., melting between 66 and 52 km). In all other cases, the initial and final melting pressure values are  $> 2$  GPa; thus, considering the lithospheric thickness beneath the Pannonoan basin, they indicate magma generation in the sublithospheric mantle. Generation of the primary magmas started predominantly at around 3 GPa, i.e., at 100 km depth. This corresponds with a depth of the spinel–garnet transitional field (Robinson and Wood 1998; Klemme and O'Neill 2000; Klemme 2004). At such depth, dry peridotite could not melt up to a mantle potential temperature of 1,450 °C; therefore, the presence of water or pyroxenite/eclogite with lower solidus is expected in the source region that may lead to lower the calculated pressure (Wang et al. 2002). Nevertheless, the final depth of melting columns of the CPR basalts is between 2.1 and 2.5 GPa (70–83 km depth), what is in good agreement with the geophysically determined thickness of the lithosphere (Horváth et al. 2006) beneath the volcanic fields (Fig. 7). In addition to the usual melting depth of the CPR basalts, the alkaline basalts from Burgenland (Pauliberg and Oberpuldendorf) fall into the 3.4 and 3.8 GPa melting lines (Fig. 6a) that correspond with an onset of melting at greater depth (110–125 km). This fits, however, well with the deep structure beneath these basaltic volcanoes, i.e., they are located in an area characterized by thick lithosphere (ca. 110 km present-day thickness; Fig. 7). The relatively shallow melting column beneath the Perşani volcanic field (86–70 km depth interval) seems to be remarkable, since formerly Dérerova et al. (2006) and Horváth et al. (2006) suggested a thick lithosphere here (about 140 km). However, Harangi et al. (2013) pointed out that the Perşani basaltic magmas were originated by melting of asthenospheric mantle and therefore the LAB should be much shallower, i.e., not deeper than 60 km. This is consistent with the geophysical result of Martin et al. (2006) and implies that a narrow rupture could have developed in the lower lithosphere beneath the Perşani area, probably as a result of the dragging effect of the descending dense lithospheric slab beneath the Vrancea zone located about 100 km from the volcanic field (Harangi et al. 2013). In two cases (Putikov vřšok and Lucaret), we got a melting column fairly deep in

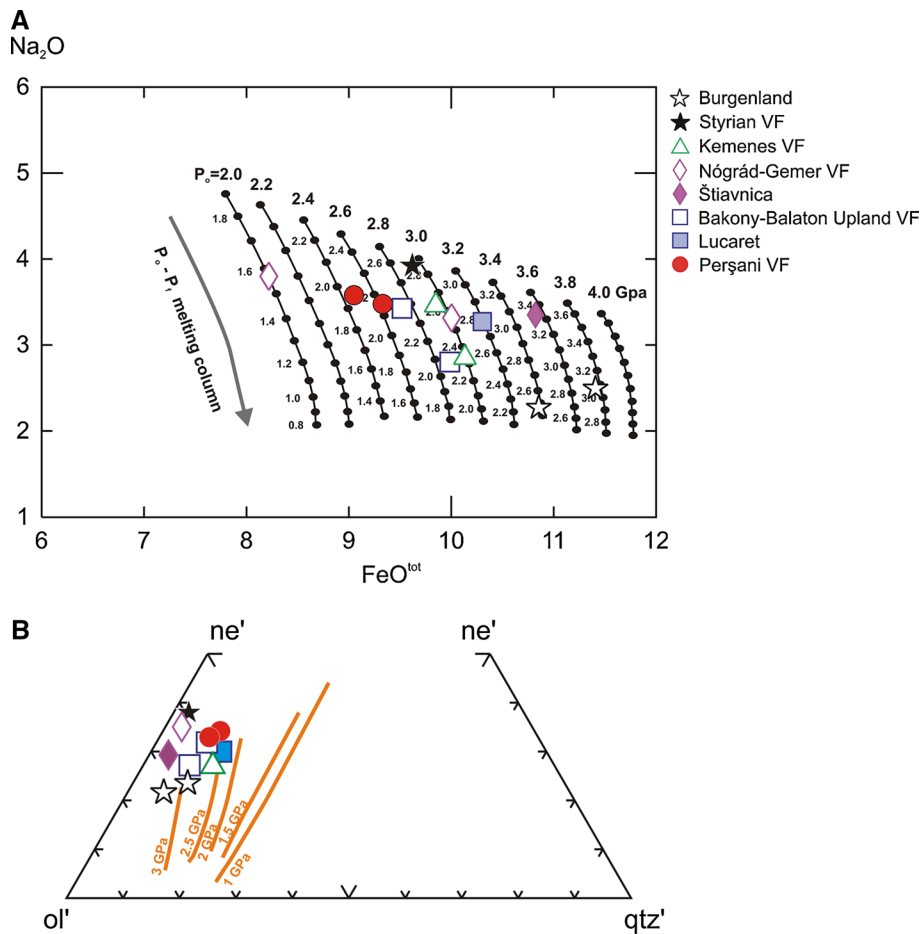


**Fig. 6 a** Estimation of the initial and final pressures ( $p_o$  and  $p_f$ , respectively) of the melting column for selected CPR basalts using the adiabatic decompression model of Langmuir et al. (1992). The  $FeO^I$  and the  $Na_2O$  of the calculated primary magmas of the CPR basalts yield information on the initial melting pressure and the cessation of the melting, i.e., the final melting pressure. Each curve represents polybaric mantle melting lines with different initial melting pressure, i.e., where the ambient mantle temperature intersects the

solidus. Each tick mark represents 0.1 GPa of decompression. The compositions of the primary magmas at the melting curves provide the values of the final pressure. **b** Determination of melting pressure based on the calculated primary magma compositions of the CPR basalts using the  $ol'-ne'-qtz'$  plot of Hirose and Kushiro (1993).  $ol' = ol + 0.75opx$ ;  $ne' = ne + 0.6ab$ ;  $qtz' = qtz + 0.4ab + 0.25opx$ , where  $ol$ ,  $opx$ ,  $ne$ ,  $ab$  and  $qtz$  are CIPW normative mineral components. Melting pressure lines are after Sakuyama et al. (2009)

comparison with the lithospheric thickness. Partial melting could start here deeper than 100 km and terminated shortly after 10–15 km mantle upwelling. A possible explanation for this would be the exhaustion of the fusible material such as hydrous peridotite or garnet-pyroxenite/eclogite.

An independent test of the result provided by the Langmuir et al. (1992) model can be achieved with comparison of the primary magma compositions of the CPR basalts with experimental data sets (Sakuyama et al. 2009) and using other geobarometric calculations (Scarrow and Cox 1995; Lee et al. 2009). Sakuyama et al. (2009) compiled results of various melting experiments and suggested that  $SiO_2$  content of the primary melt is the most sensitive parameter on melting pressure in the range of 1.0–3.0 GPa and it does not depend significantly on the degree of melting, the initial bulk composition and modal mineralogy. Water content of

the source peridotite could slightly increase the  $SiO_2$  content of the melt at constant pressure (Hirose and Kawamoto 1995) that may lead to slight underestimation of the pressure if dry peridotite melting is considered. Plotting the primary magma compositions of the CPR basalts on the  $ol'-ne'-qtz'$  triangular diagram along with the isobaric melting lines as determined by Sakuyama et al. (2009) based on experimental data sets, 2.5–3.5 GPa melting pressures are obtained (Fig. 6b) that are in good agreement with the constraints on the melting columns described above, particularly with the initial melting pressure. The only exception is the basalts from Lucaret for which we got melting pressure of 2.5 GPa, significantly lower than from the Langmuir et al. (1992) model (3.20–2.75 GPa). Scarrow and Cox (1995) developed a simple equation for the melting pressure estimate based on the  $SiO_2$  content of primary rocks. It gives slightly lower

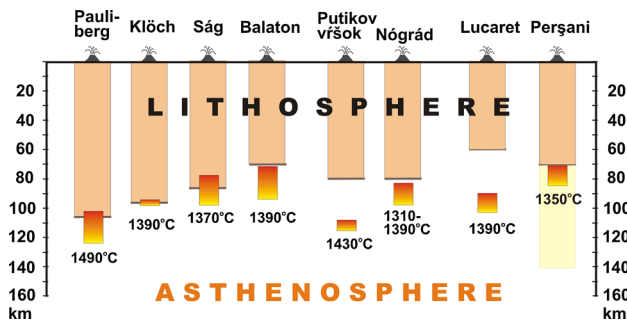


**Fig. 7** Calculated melting columns for different basalts (based on Langmuir et al.'s (1992) model) compared with the present lithosphere–asthenosphere boundary (LAB) beneath the volcanic fields that is inferred from interpretation of seismic data (Horváth et al. 2006). Mantle potential temperatures are given using the calculation scheme of Lee et al. (2009) using molar  $Fe^{3+}/Fe^{tot} = 0.13$ . Beneath the Perşani volcanic field Dérerova et al. (2006) and Horváth et al. (2006) suggested a thick lithosphere (about 140 km), whereas Martin et al. (2006) indicated much thinner lithosphere. Our melting column calculation for the Perşani basalts is consistent with the proposed lithosphere thickness of Martin et al. (2006)

pressure values than the  $ol'-ne'-qtz'$  diagram, whereas the corrected  $SiO_2$  geobarometer by Wang et al. (2002) appears to strongly overestimate the pressure particularly at higher pressure ( $>2.5$  GPa). Finally, we applied also the peridotite-melt barometer of Lee et al. (2009), which gives consistent result with the  $SiO_2$  barometer of Scarrow and Cox (1995), but also with the final pressure estimate of the Langmuir et al. (1992) model (Fig. 8). There is also a good correlation between the pressure obtained by the Lee et al. (2009) barometry and the  $qtz'/(ol'-ne'-qtz')$  ratio, which was suggested as a sensitive parameter of depth of melting (Sakuyama et al. 2009). The only exception is the basalts from Pauliberg that form a parallel trend at slightly higher pressure range, probably due to the difference of the source lithology.

In summary, we can conclude that melting of the upwelling asthenospheric mantle material could start at about 100 km depth beneath most of the volcanic fields of the CPR, and the final melting pressure could have been controlled by the thickness of the lithosphere, i.e., the LAB. Partial melting occurred at greater depth beneath Pauliberg, which is underlain by thicker lithosphere, whereas beneath the Perşani area melting could have taken place at shallower depth due to a local rupture of the lower lithosphere. The youngest basalt beneath Putikov vřšok generated at greater depth (100–120 km), whereas the 2.4 Ma Lucaret basalt could have been derived also from a relatively shallow depth in spite of the higher FeO content of the basalts.

#### Conditions of melt generation

We proposed that partial melting of the upwelling asthenospheric mantle material could lead to the generation of

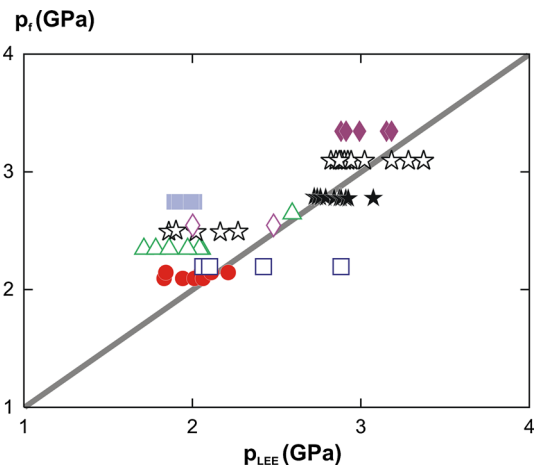


**Fig. 8** Comparison of the melting pressure obtained by the calculation procedure of Lee et al. (2009) with the final melting pressure ( $p_f$ ) provided by the Langmuir et al. (1992) model. There is a reasonably good correlation between these pressure values. Symbols as in Fig. 2

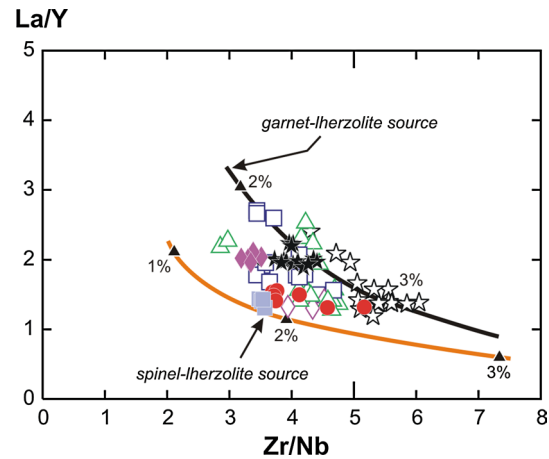


**Fig. 9** Trace element modeling for the melt generation of the CPR basaltic magmas. Model parameters: critical melting model (critical melt fraction is 0.01) proposed by Sobolev and Shimizu (1992) with the following source rocks: spinel-lherzolite—olivine (57 %), orthopyroxene (25.5 %), clinopyroxene (15 %), spinel (2.5 %); garnet-lherzolite—olivine (60.1 %), orthopyroxene (18.9 %), clinopyroxene (13.7 %), garnet (7.3 %). Melting modes are  $ol1.21opx8.06cpx76.37sp14.36$  for spinel-lherzolite and  $ol1.30px8.7cpx36gt54$  for garnet-lherzolite, respectively. Source rock composition: La and Nb— $4 \times$  primitive mantle values (2.59 and 2.63 ppm, respectively), Zr— $2 \times$  primitive mantle values (21 ppm) and Y— $1.5 \times$  primitive mantle values (6.45 ppm, where primitive mantle values are from McDonough and Sun 1995). Distribution coefficients are from Kostopoulos and James (1992). Tick marks indicate the degree of melting at each melting model. Symbols are explained in Fig. 2

basaltic magmas, which fed the volcanic eruptions in the monogenetic volcanic fields of the CPR. A further constrain on the melt generation process can be obtained from trace element petrogenetic modeling (Fig. 9). We used

different initial compositions (depleted MORB mantle and slightly enriched primitive mantle; Salters and Stracke 2004; McDonough and Sun 1995) and different mineralogical assemblage (garnet-lherzolite, spinel-lherzolite) of the source material and different melting models (batch and fractional melting; Shaw 1970; critical or dynamic melting; Sobolev and Shimizu 1992; Zou 1998; Shaw 2000) with the mineral-melt distribution coefficients proposed by Kostopoulou and James (1992). Trace element ratios of Zr/Nb and La/Y were chosen, because their values are not dependant on early-stage crystal fractionation and are sensitive (La/Y) on the presence of spinel and garnet in the mantle source. As we discussed earlier, it is unlikely that amphibole was also present in the source region of the CPR basalts, and therefore, it was not considered in the modeling calculations. The result of the petrogenetic modeling is shown in Fig. 9.

The primary magmas of the CPR basalts were formed from trace element-enriched mantle source (1.5–4.0 times of the primitive mantle composition; McDonough and Sun 1995) within the spinel–garnet transitional zone (Fig. 9). The degree of melting is somewhat model dependant, but it is between 1.5 and 5 %. The best fit of the CPR basalts with the melting model lines is given assuming continuous dynamic melting or decompressional critical melting (Sobolev and Shimizu 1992; Zou 1998; Shaw 2000) process. This model is consistent with the melting process described in the previous section, i.e., commencing of melting in a mantle source, where garnet prevails over spinel and then continues in the spinel-stability field. In this case, 2–3 % melting is required to obtain the composition of the primary basaltic magmas of the CPR. Noteworthy, the Lucaret basalts fall on the spinel-peridotite melting line implying shallow melting and suggest that the FeO content of the bulk rock overestimates the melting pressure and the SiO<sub>2</sub>-based geobarometries provide more reliable result. On the other hand, the basalts from the western Pannonian basin (Pauliberg, Oberpullendorf and Klösch from the Styrian basin) fall on the garnet-peridotite melting line consistent with their derivation from a deeper source.

The depth of melting for the CPR basalts as shown by various models is between 60 and 120 km. The associating melting temperature can be determined using the peridotite-melt thermometer by Lee et al. (2009; using molar  $\text{Fe}^{3+}/\text{Fe}^{\text{tot}} = 0.13$ ) and the PRIMELT2 software of Herzberg and Asimow (2008; using  $\text{Fe}_2\text{O}_3 = \text{TiO}_2$ ). They resulted in fairly similar temperature values up to 1,470 °C (Fig. 7), where the Lee et al.'s (2009) calculation tends to give much higher (>100 °C) temperature than the PRIMELT2 (mostly for the Pauliberg basalts). The lowest mantle potential temperature is shown by the Perşani basalts (1,310–1,380 °C) that records indeed shallow melting as indicated by the geobarometric calculations, whereas in the other volcanic

fields, we got melting temperature in a range between 1,350 and 1,450 °C. The highest potential temperature values were obtained for the basalts at Pauliberg (>1,440 °C) and at Putikov vřšok (1,420–1,450 °C).

Taken together the obtained pressure and temperature values, the Fig. 10 shows that the melting columns of the basaltic magmas of the CPR are just below the dry peridotite solidus. This requires either some water or a more fusible material, such as pyroxenite or eclogite in the mantle source. The relatively low CaO content (<10 wt%) of the calculated primary basaltic magmas and the low Ca also in the olivine phenocrysts (Harangi et al. 2013) are features that can be explained by pyroxenite melting (Herzberg 2011). However, the olivine in the CPR basalts (Embey-Isztin and Dobosi 2007; Jankovics et al. 2012, 2013; Harangi et al. 2013) has relatively low Ni and high Mn concentrations that is just the opposite of what required in the case of pyroxenite melting (Sobolev et al. 2007). These features could be explained, however, also by the lid-effect, i.e., by variations in lithospheric thickness (Niu et al. 2011). Magmas generated under a thin lithosphere could crystallize olivines with relatively low Ni and high Mn and corresponding low Ni/Mg, low Ni/(Mg/Fe) and high Mn/Fe and high Ca/Fe ratios. Although the Ca deficiency of the olivine and the host rocks of the CPR is still unresolved, it appears that the basaltic magmas beneath the CPR could have originated dominantly from a peridotitic mantle source. In this case, however, some water (50–200 ppm; Hirschmann et al. 2009) should be present in the source region. The origin of this volatile content can be explained either by the supposed intense Palaeogene–Miocene subduction around the Carpathians (Csontos et al. 1992) or dewatering of the accumulated subducted material in the transitional zone (Hetényi et al. 2009). An important point coming from the Fig. 10 is that the upper mantle beneath the thin continental lithosphere of the Pannonian basin has a temperature close to the peridotite solidus and the mantle could be partially hydrous that makes it potentially still fusible. Eruptions of basaltic magmas in the last 2 Ma could confirm the potentially fusible state of the mantle. The low seismic velocity anomaly down to the transitional zone beneath the northern part of the Pannonian basin (Dando et al. 2011) could provide a further supporting evidence of this.

#### Mantle source characteristics

Chromian spinels enclosed by olivine phenocrysts could provide important information about the mantle sources of the CPR basalts. They occur in each volcanic field, and therefore, it can be used to gain insights into the nature of the sublithospheric mantle on a regional scale. Chromian spinel is often the liquidus phase along with olivine in basaltic melts (Fisk and Bence 1980; Luhr and Carmichael

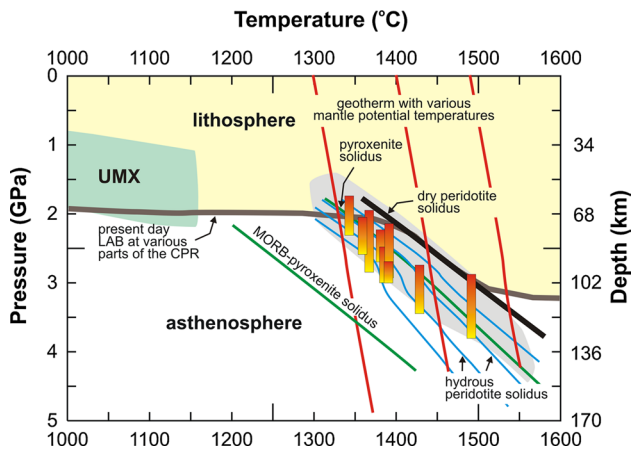


**Fig. 10** Melting conditions beneath the Carpathian–Pannonian region in a pressure–temperature diagram. The position of the melting columns is based on the result of the Langmuir et al.’s (1992) model combined with the mantle potential temperature and melting pressure values calculated by the thermobarometer of Lee et al. (2009). The melting columns of the basaltic magmas are just below the dry peridotite solidus (as defined by Hirschmann 2000). This requires either some water or a more fusible material, such as pyroxenite or eclogite in the mantle source. Hydrous peridotite solidi: Hirschmann (2006); pyroxenite (MIX1G) pyroxenite solidus: Kogiso et al. (2003); MORB-like pyroxenite solidus: Pertermann and Hirschmann (2003). UMX: position of the ultramafic peridotite xenoliths as given by Embey-Isztin et al. (2001) and Kovács et al. (2012)

1985); therefore, it reflects the primary characteristics of the basaltic melt. It can be used for deciphering the original magmatic characteristics even of heavily altered basalts (Allan 1992). Composition of the liquidus spinels is considered to be close to that of the spinels in the residual mantle source region, although other controlling factors such as magma differentiation, crystallization pressure, redox condition and the degree of partial melting also influence the composition of spinels (Hill and Roeder 1974; Sigurdsson and Schilling 1976; Dick and Bullen 1984; Allan et al. 1988; Roeder and Reynolds 1991; Arai 1994; Clynne and Borg 1997; Kamenetsky et al. 2001; Roeder et al. 2003).

The spinel inclusions found in the CPR basalts show a wide compositional range (Cr-number = 0.15–0.68, Mg-number = 0.2–0.8). They are mostly chromian spinels thought to be formed as early-stage mineral phases; however, as soon as they became out of the narrow temperature interval where they could appear as liquidus crystals (Sigurdsson and Schilling 1976; Fisk and Bence 1980; Luhr and Carmichael 1985), they react with the differentiated melt and the spinel component is rapidly replaced by magnetite and ulvöspinel components increasing their FeO and Fe<sub>2</sub>O<sub>3</sub>, and TiO<sub>2</sub> contents (Luhr and Carmichael 1985; Clynne and Borg 1997; Arai 1992; Roeder et al. 2003). Therefore, we selected spinels enclosed by the most magnesian (Fo >84 mol%) olivines, and then, we filtered

out the analyzed spinel compositions using their TiO<sub>2</sub> and Fe<sup>3+</sup>-number in order to focus on the most primitive spinel population. Instead of using a definite limit of these parameters (e.g., Clynne and Borg 1987), we plot all the data on the Cr–Fe<sup>3+</sup>–Al triangular diagram and compared them with the natural basalt-hosted spinel compositional range (Barnes and Roeder 2001). The majority of the MORB spinels show a wide variation in the Cr–Al trend, whereas many spinels from OIB have a slight enrichment in Ti and Fe. We selected the spinel population thought to represent liquidus mineral phases primarily based on the overlap with the 50th percentiles of the OIB and MORB spinels, and then, we considered the possible differentiation trends. The whole data set and the selected “liquidus-spinel” compositions are shown in Fig. 11. The primary spinels form four coherent groups in the Cr–Fe<sup>3+</sup>–Al diagram that could represent different mantle domains beneath the CPR. Three of them appear in all major volcanic fields of the CPR, whereas the fourth one belongs solely to the Pauliberg location. In general, spinel composition closely mimics the host rock composition (as shown by the correlation between the Cr-number of spinels and the Fe<sub>2</sub>O<sub>3</sub>, Al<sub>2</sub>O<sub>3</sub> and TiO<sub>2</sub> contents of the host rock). The basanites of Pauliberg have a specific composition within the Miocene–Quaternary alkaline basalts of the CPR (Embey-Isztin and Dobosi 1995; Ali and Ntaflou 2011), showing depletion in Al and enrichment in Fe and Ti compared with the others. Spinel in these rocks are also depleted in Al (thus, they have relatively high Cr-number) and slightly enriched in Fe and Ti, plotting outside from the MORB and OIB spinel fields. Nevertheless, considering the specific composition of their host rock, they could also belong to the “liquidus-spinel” population and reflect a particular mantle source region of the Pauliberg magmas. Tentatively, this might be a sign of involvement of eclogite during melting, a hypothesis that requires further studies.

Compositional characters of the spinels are controlled by many factors as listed before. Influence of the magma differentiation could be filtered out by limiting the data set to the most primitive spinels. The pressure of crystallization affects predominantly the Al content of the chromian spinels (Dick and Bullen 1984), showing positive correlation between them. The large compositional variation of the spinel compositions in the CPR basalts, however, could be unlikely related to the variable crystallization pressures, since the lowest Al content in spinels was recorded in those basalts which were interpreted as derived from the deepest source (Pauliberg, Putikov, Lucaret). Spinel composition is dependant also on the degree of partial melting as demonstrated by Arai (1994) and Baker and Stolper (1994). The Cr-number of spinel in the mantle restite rock increases with increasing degree of melting. Spinel with 0.10–0.15 Cr-number are considered to represent

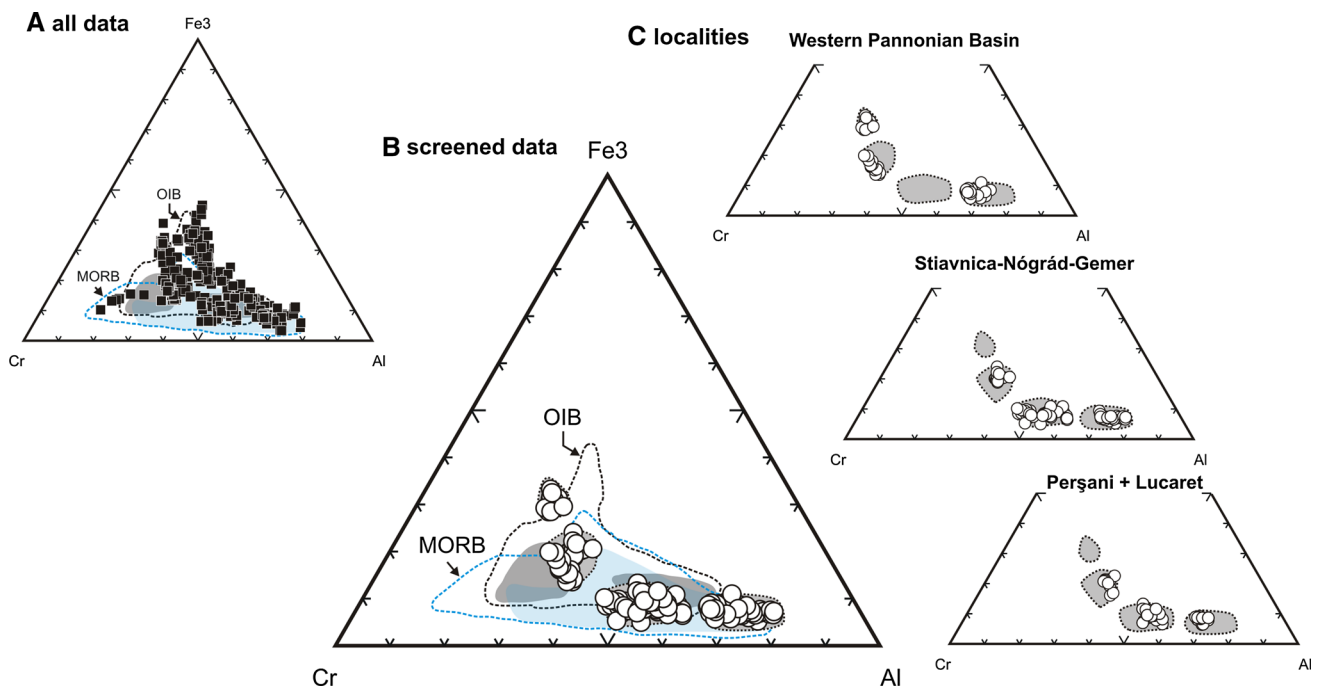


**Fig. 11** Compositional characteristics of spinel inclusions in olivine phenocrysts of the CPR basalts based on the Cr–Fe<sup>3+</sup>–Al diagram. The most primitive spinels form four compositionally coherent groups that can be related to the existence of different mantle domains in the source regions of the basaltic magmas. Note that three

of these groups are present beneath each volcanic fields of the CPR. MORB and OIB spinel fields are as defined by Barnes and Roeder (2001). Compositional data of spinels are from Jankovics et al. (2012), Harangi et al. (2013); Sági and Harangi (2013)

fertile mantle regions, whereas spinels with Cr-number of about 0.6 could indicate more than 25 % degree of melting (Baker and Stolper 1994). However, no correlation can be recognized between the variation of spinel Cr-number and the incompatible trace element ratios of the CPR basalts that are sensitive on the progressive melting process (e.g., La/Y, [Sm/Yb]<sub>N</sub>). Furthermore, our petrogenetic model calculation suggests that the mafic magmas of CPR could have originated by 2–3 % of melting, and therefore, the large compositional variation of spinels cannot be attributed to various degrees of partial melting. Taking all of these into account, we can conclude that the spinels in the CPR basalts reflect the nature of the mantle source region, more precisely the character of the residual mantle rocks, and indicate heterogeneous, variably depleted sublithospheric mantle beneath the Pannonian basin.

Spinel compositions suggest that at least three main compositional domains (and a specific one beneath Pauliberg) could exist in the mantle source region and they are well distributed beneath each volcanic field. Although the composition of the liquidus spinels is close to the spinels in the restitic mantle rocks rather than in the initial source material, the small degree of melting characterizing the CPR basalts could not significantly modify the compositional feature of the initial spinels as also emphasized by Clyne and Borg (1997) for the Lassen basalts.

Therefore, the composition of the restite spinels could be close to that of the initial ones. Noteworthy, the youngest (<600 ka) basalts could have derived either from the most fertile mantle source domain (Perşani basalts; spinel Cr-number = 0.23–0.32; Harangi et al. 2013) or from a mantle domain akin to enriched OIB (Putikov vršok; spinel Cr-number = 0.55–0.61; TiO<sub>2</sub> = 2.0–3.5 wt%; Sági and Harangi 2013). This might mean that the sublithospheric mantle beneath CPR could be potentially still capable to produce basaltic magmas, i.e., contains fusible parts of material.

#### Geodynamic relationships

The origin of the alkaline basaltic volcanism in the CPR seems to be enigmatic since it occurred after the main phase of the lithospheric extension of the Pannonian basin (20–15 Ma; Horváth et al. 2006), during the stage of post-rift thermal subsidence and tectonic inversion. Melt generation has taken place intermittently since 11 Ma with a peak period between 5 and 1 Ma. In such situations, hot mantle upwelling beneath the thinned lithospheric realm seems to be a viable mechanism to produce low-volume basaltic magma (Embey-Isztin et al. 2001; Harangi 2001b). Composition of the Neogene alkaline mafic rocks in Europe shares many similarities, particularly in the radiogenic isotope

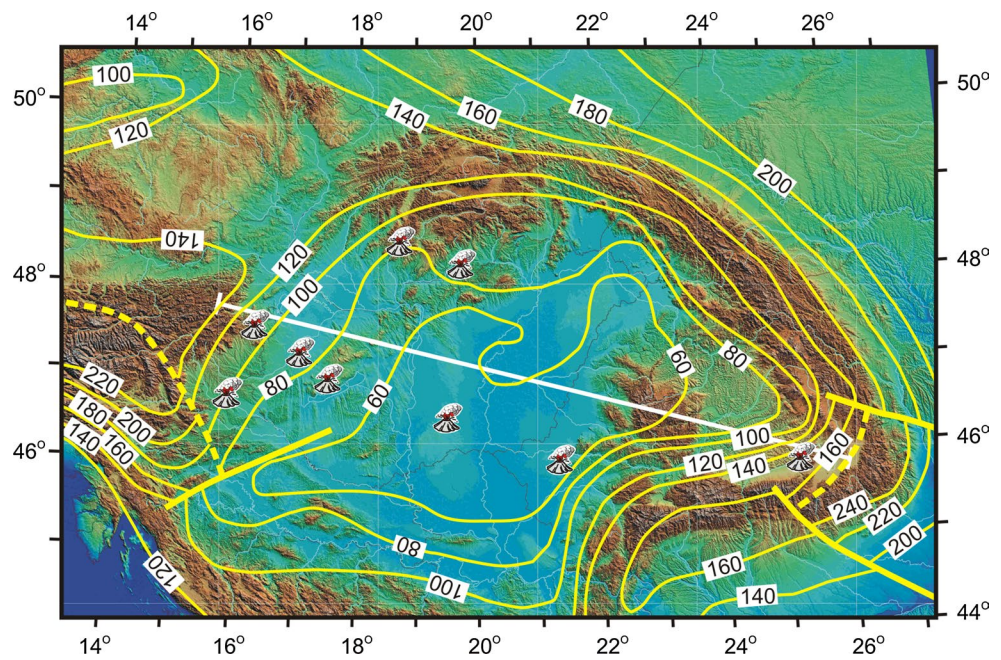
ratios. Taking this into account and correlating it with seismic anomalies in the sublithospheric mantle beneath Europe, Hoernle et al. (1995) and Granet et al. (1995) proposed a common mantle reservoir of the mafic magmas (called European Asthenospheric Reservoir; EAR by Cebriá and Wilson 1995) that fed the basaltic volcanism via localized active mantle plumes (“plume finger”) in different parts of Europe, such as in the Massif Central, the Rhenish area, the Eger graben, Bohemia and also in the Pannonian basin (Granet et al. 1995; Wilson and Patterson 2001). The plume finger model was put forward for the Pannonian basin by Embey-Isztin et al. (2001), Seghedi et al. (2004b) and Seghedi and Downes (2011). Seghedi et al. (2004b) distinguished at least three plume fingers beneath the CPR, primarily based on the HIMU-like isotopic character of the basalts. However, we have to emphasize that the HIMU-like isotopic ratios have solely a descriptive message and this does not necessarily mean plume origin. Nevertheless, the plume-related basaltic magmatism in the CPR was proposed also by other authors based on geological, geochemical and geophysical considerations (Goes et al. 1999; Buikin et al. 2005; Burov and Cloetingh 2009). In contrast, Harangi and Lenkey (2007) argued against a mantle plume beneath the Pannonian basin.

There are a couple of observations that are not consistent with the plume model. Beneath the Pannonian basin, in the depth range of 400–650 km, a positive seismic velocity anomaly is recognized (Wortel and Spakman 2000; Piro-mallo et al. 2001; Piro-mallo and Morelli 2003; Hetényi et al. 2009). The origin of this anomaly was postulated as accumulation of thick, cold material, possibly subducted residual material supplied from several subduction episodes (Peninetic in the Cretaceous, Vardar in the Palaeogene, and the East Carpathian subduction in the Miocene; Hetényi et al. 2009). This vast amount of cold material can form a barrier against the rise of any lower mantle-derived plume and prevents the initiation of upwelling of hot material from the Transition Zone. However, it has been shown that the transitional zone could be one of the wettest parts of the upper mantle, particularly when subducted material is accumulated there for a long time (Hirschmann 2006; Karato 2011). Thus, it could serve as the source for wet plumes instead of hot plumes. In this scenario, wet melting in the upper part of the transition zone (Hirschmann 2006) could provide small volume hydrous magmas that initiate further melting beneath the continental lithosphere. Although this is a reasonable scenario, it does not explain the observation why the basaltic volcanic fields are at the marginal parts of the Pannonian basin and not in the central areas. The characteristic features of hot mantle plumes are also missing in the CPR. The broad topographic updoming such as detected in the Massif Central (Wilson and Patterson 2001), or in classic hot spot areas (Courtilot et al. 2003), is absent; on the

contrary, some parts of the Pannonian Basin are still subsiding. The high heat flow in the CPR (Lenkey et al. 2002) can be readily explained by the thinning of the lithosphere during basin formation and by the still shallow asthenosphere (Royden et al. 1982). As far as the HIMU-like isotopic ratios of some CPR basalts are concerned, they could have also a metasomatic origin (e.g., Hart 1988; Sun and McDonough 1989; Halliday et al. 1995; Pilet et al. 2005). The sporadic distribution and the low-magma output type of the volcanic fields in the CPR also do not support any hot mantle plume origin. Therefore, there are no supporting evidences that favor hot mantle plume or plume finger (Seghedi et al. 2004a, b) origin of the basaltic volcanism in the CPR.

Generation of basaltic magmas in the asthenosphere requires upward movement of solid mantle material, i.e., a mantle flow. In this context, the spatial distribution of the basalt volcanic fields at the peripheral areas of the CPR could have relevance. They occur above a LAB with sharp depth variation between the orogenic Alps and cratonic North European Platform with thick (>160 km) lithospheric roots and the stretched Pannonian basin with thin (<70 km) lithosphere within relatively short distances (Fig. 12). The Pannonian basin could therefore act as a thin-spot providing suction in the sublithospheric mantle and generating mantle flow from below the thick lithospheric roots (Harangi and Lenkey 2007; Harangi 2009). The SKS splitting measurements show a dominant west–east direction beneath the western part of the Pannonian basin with a clear continuation from the Alps, and this direction changes to a northwest–southeast trend toward the central and northern areas (Kovács et al. 2012). On the western side of the Alps, similar, east- to west-directed SKS splitting directions were recognized that turn gradually in north–south direction northward and this was considered as relatively recent asthenospheric flow (Barruol et al. 2011). Remarkably, a similar seismic pattern was observed also in the Lake Baikal area, where it was interpreted as sublithospheric mantle flow from beneath the thick Siberian craton toward the thin Baikal–Mongolian area (Lebedev et al. 2006). The low-volume, scattered and sporadic basalt volcanism in the Baikal rift could have been connected with this mantle flow by decompression melting when the asthenospheric material ascended from the 200 km depth beneath the craton to shallower depths beneath the rift (Lebedev et al. 2006). A similar triggering mechanism was put forward by Niu (2005) explaining the basaltic volcanism in the East China lowland. Thus, it appears that a large contrast in the LAB architecture could enhance mantle flow that results in intra-plate basaltic volcanism with many similarities to OIB-type compositions. This appears to be the case also in the Alps–Pannonian basin transition zone, where relatively hot asthenospheric material could ascend from beneath the Alps along the steep LAB (Harangi 2009; Fig. 13). The

**Fig. 12** Position of the basalt volcanic fields in the CPR compared with the seismically defined lithosphere–asthenosphere boundary lines (Horváth et al. 2006). Note that the volcanic fields are located at the margin of the Pannonian basin and not in the central parts where the lithosphere is the thinnest



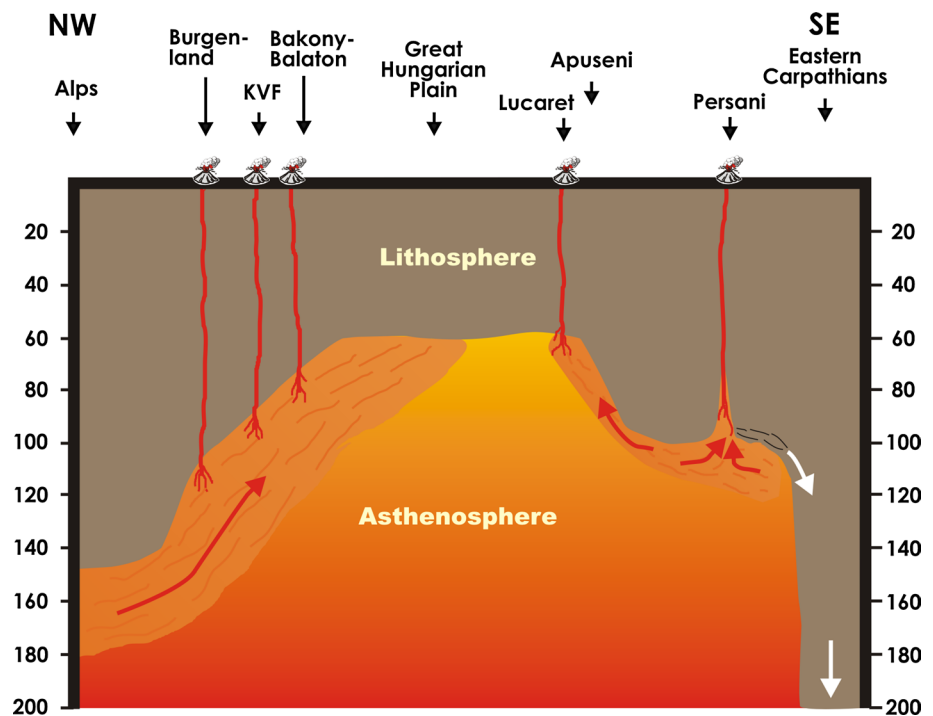
important role of asthenospheric mantle flow as a driving force for the Neogene extension and extrusion events is getting to have an increasing attention in the geodynamic model of the Pannonian basin. Konečný et al. (2002) invoked an asthenospheric flow due to subduction rollback mechanism and explained the magma generation by this process. Kovács et al. (2012) proposed that this mantle flow is the result of the convergence between the Eurasian and African plates along the Alpine belt, whereas Horváth and Faccenna (2011) suggested that mantle material was pumped through the Istria slab window beneath the CPR mantle as a result of slab rollback along the eastern margin of the region. An important difference between these models and the explanation put forward in this paper is the time of the mantle flow. According to Konečný et al. (2002), Kovács et al. (2012) and Horváth and Faccenna (2011), this process could have been taking place since the Oligocene/Miocene and act as a major role in the geodynamic evolution of the CPR, whereas here we propose that it is a passive process commenced just after the Mid-Miocene formation of the Pannonian basin with strongly thinned lithosphere, and in this case, this thin-spot condition acted as a driving force of the mantle flow.

In the northern part of the Pannonian basin, there has been a long-lasting volcanic activity since about 16 Ma (Harangi et al. 2007). The alkaline basalt volcanism followed an intense calc-alkaline volcanic period (Konečný et al. 1995, 2002). Nevertheless, no traces of subduction-related mantle source are observed in the composition of the basaltic products. It can be explained by effective change in the sublithospheric mantle beneath the Štiavnica and Nógrád–Gemer area that could require again mantle

flow mechanism. In the seismic tomography model sections published by Dando et al. (2011), a low-velocity anomaly can be observed beneath this region that has a continuation into the deeper mantle toward north. Tentatively, this can be interpreted as a sign of an upward flow beneath the steep LAB. The low-magma output and the sporadic eruption events over several million years long period (8–0.1 Ma) could suggest, however, a tectonic control of the melt generation–magma ascent processes. Strain localization in the upper mantle beneath major faults that penetrate the upper mantle (Leloup et al. 1995; Vauchez et al. 2012) could be a possible mechanism of this. Reactivation of transensional tectonic lines could have a close link with the tectonic inversion of the Pannonian basin (Horváth and Cloetingh 1996) that started in the Late Miocene when the peak magma output phase occurred in the Bakony–Balaton Upland and the Štiavnica and Nógrád–Gemer volcanic fields. Further research could focus on the interrelationship of tectonic processes along preexisting lines and the volcanic events.

The youngest basalt volcanic field was developed at the eastern part of the CPR (Perşani area; Seghedi and Szakács 1994; Downes et al. 1995) from 1.2 to 0.6 Ma (Panaiotu et al. 2013). Seghedi et al. (2011) invoked toroidal asthenospheric flow around the downgoing slab beneath Vrancea to explain the localized alkali basalt volcanism, whereas Harangi et al. (2013) proposed that this could have occurred as a response to the formation of a narrow rupture in the lower lithosphere, possibly as a far-field effect of the dipping of dense continental lithospheric material beneath the Vrancea zone. Upper crustal extensional stress field with reactivation of normal faults at the eastern margin of

**Fig. 13** Conceptual model for the triggering of melt generation beneath the Pannonian basin. See text for explanation



the Transylvanian basin could enhance the rapid ascent of the mafic magmas.

Finally, it is remarkable that local low-velocity mantle anomaly has been detected beneath both the Štiavnica and the Perşani areas (Dando et al. 2011; Popa et al. 2012) that along with our interpretation about the presence of mantle region containing still fusible material suggest that further volcanic eruptions cannot be unambiguously excluded in these areas. The rapid ascent of the magmas (Harangi et al. 2013; Jankovics et al. 2013) implies that the quiet situation could change rapidly.

### Summary

Evaluation of the major and trace element content of the most primitive basalts in the CPR along with the interpretation of the most primitive spinel compositions indicates that the primary magmas could have generated in the convective asthenosphere. Trace element modeling indicates incompatible trace element-enriched source composition and 2–3 % melting within the garnet–spinel transition zone. Melting started at about 100 km depth where garnet prevails over spinel and continued usually up to the base of the lithosphere. Thus, the final melting pressure could indicate the ambient LAB. The asthenospheric mantle source regions of the basalts were heterogeneous, presumably at small scale. Spinel compositions show a wide range, although four coherent groups can be distinguished that are interpreted as reflect the main mantle domains beneath this region. They can be

recognized at almost each volcanic field. Two of these have fertile and slightly depleted character, respectively, whereas the two others are enriched in Fe and Ti and overlap the spinels found in the basalts of Hawaii. They might indicate involvement of pyroxenitic/eclogitic lithology in the melting process that requires further investigation. Major element composition of some of the basalts (low Al and high Ti and Fe; e.g., Pauliberg, Putikov) could be also consistent with melting of carbonated, silica-deficient eclogite. Indeed, considering the depths of the estimated melting columns of the CPR basaltic magmas, a more fusible material than the dry peridotite is required in the source regions of the magmas. The presence of water or pyroxenite/eclogite could explain melting at such depth.

The prevailing estimated mantle potential temperature (1,300–1,400 °C) along with the number of further observations does not require anomalously hot asthenospheric mantle. Thus, we can exclude the presence of any mantle plume or mantle plume fingers beneath the Pannonian basin. The locations of the monogenetic basalt volcanic fields at the western and northern margin of the Pannonian basin could indicate a close relationship with the steep LAB beneath these areas. We propose that asthenospheric flow from beneath the adjoining thick lithospheric domains (Alps, cratonic North European Platform) to the thinned Pannonian basin could play a triggering role in the melt generation. A near-vertical upwelling along the steep LAB could result in decompressional melting producing low-volume melts. The Pannonian basin could therefore act as a thin spot after the Mid-Miocene syn-rift phase (20–12 Ma)

and provided suction in the sublithospheric mantle generating asthenospheric flow from below the thick lithospheric roots. In addition to this dominant process, single basaltic volcanic events in the inner part of the Pannonian basin could have been related to strain localization in the upper mantle beneath major strike-slip faults that penetrate the upper mantle. Further southeast, close to the Vrancea zone, the youngest basalt volcanic field in the CPR could have been formed as a plate tectonic response of the dipping dense continental lithospheric material. The suction of the descending lithospheric slab could result in narrow rupture at the base of the lithosphere. Decompression melting of the upwelling asthenospheric mantle could result in magma generation, while reactivation of normal faults enhanced the rapid ascent of the magmas.

Origin of basaltic magmas with fairly primitive composition for the last 1 Ma implies that fusible material could still exist in the mantle, which have a potential temperature close to the solidus. This inferred condition and the low-velocity anomalies detected in the mantle depths as well as the still high localized heat flows in these areas all suggest that continuation of the basaltic volcanism in the CPR cannot be unambiguously excluded.

**Acknowledgments** Our ideas about the basaltic volcanism in the CPR have refined during the number of instructive and sometimes heavy discussions with several colleagues such as Hilary Downes, Theodoros Ntafllos, Ioan Seghedi, Frank Horváth, Károly Németh, Csaba Szabó, István Kovács, Orlando Vaselli, László Lenkey, Marge Wilson, Michele Lustrino, Jaroslav Lexa, Kadosa Balogh, Zoltán Pécskay and László Fodor. These were promoted by great workshops started with the PANCARDI meetings in the 1990s and early 2000s, followed by the ILP PLUME workshop at Mt. Sainte-Odile in 2006, the EMAW conference in Ferrara in 2007 and the Basalt 2013 in Görlitz in 2013. Discussions about the mantle potential temperature calculations with Claude Herzberg and Keith Putirka were particularly stimulated. Terry Plank kindly provided the calculation scheme of the Langmuir et al.'s (1992) melting model. Participation of the young scientists, M. Éva Jankovics, Balázs Kiss and Réka Lukács, was supported in this research by the European Union and the State of Hungary, co-financed by the European Social Fund in the framework of TÁMOP-4.2.4.A/2-11/1-2012-0001 "National Excellence Program". Constructive comments provided by Stefan Jung and an anonymous reviewer helped us to clarify our views.

## References

- Aldanmaz E, Koprubasi N, Gurer ÖF, Kaymakci N, Gourgaud A (2006) Geochemical constraints on the Cenozoic, OIB-type alkaline volcanic rocks of NW Turkey: implications for mantle sources and melting processes. *Lithos* 86:50–76
- Ali S, Ntafllos T (2011) Alkali basalts from Burgenland, Austria: petrological constraints on the origin of the westernmost magmatism in the Carpathian–Pannonian Region. *Lithos* 121:176–188
- Ali S, Ntafllos T, Upton BGG (2013) Petrogenesis and mantle source characteristics of Quaternary alkaline mafic lavas in the western Carpathian–Pannonian region, Styria, Austria. *Chem Geol* 337–338:99–113
- Allan JF (1992) Cr-spinel as a petrogenetic indicator: deducing magma composition from spinel in highly altered basalts from the Japan Sea, Sites 794 and 797. *Proc Ocean Drill Progr* 127(128):837–847
- Allan JF, Sack RO, Batiza R (1988) Cr-rich spinels as petrogenetic indicators: MORB-type lavas from the Lamont seamount chain, eastern Pacific. *Am Mineral* 73:741–753
- Arai S (1992) Chemistry of chromian spinel in volcanic rocks as a potential guide to magma chemistry. *Mineral Mag* 56:173–184
- Arai S (1994) Compositional variation of olivine–chromian spinel in Mg-rich magmas as a guide to their residual spinel peridotites. *J Volcanol Geotherm Res* 59:279–293
- Bada G, Horváth F, Fejes I, Gerner P (1999) Review of the present-day geodynamics of the Pannonian basin: progress and problems. *J Geodyn* 27:501–527
- Baker MB, Stolper EM (1994) Determining the composition of high-pressure mantle melts using diamond aggregates. *Geochim Cosmochim Acta* 58:2811–2827
- Balázs E, Nusszer A (1987) Unterpannonischer Vulkanismus der Beckengebiete Ungarns. *Ann Hung Geol Inst* 69:95–104
- Balogh K, Németh K (2005) Evidence for the Neogene small-volume intracontinental volcanism in the western Hungary: K/Ar geochronology of the Tihany Maar volcanic complex. *Geol Carp* 56:91–99
- Balogh K, Mihalikova A, Vass D (1981) Radiometric dating of basalt in Southern and Central Slovakia. *Zap Karpaty ser Geol* 7(113):126
- Balogh K, Jámor A, Partényi Z, Ravaszné Baranyai L, Solti G (1982) A dunántúli bazaltok K/Ar radiometrikus kora. *A Magyar Állami Földtani Intézet Évi Jelentése az 1980. évről*:243–259
- Balogh K, Árvai-Sós E, Pécskay Z, Ravasz-Baranyai L (1986) K/Ar dating of post-Sarmatian alkali basaltic rocks in Hungary. *Acta Mineralogica et Petrographica Szeged* 28:75–93
- Balogh K, Harald L, Pécskay Z, Ravasz Cs, Solti G (1990) K/Ar radiometric dating of the Tertiary volcanic rocks of East-Styria and Burgenland. *MÁFI Évi Jel.* 1988-ről:451–468
- Balogh K, Ebner F, Ravasz Cs (1994) K/Ar alter tertiärer Vulcanite de südöstlichen Steiermark und des südlichen Burgenlands. In: Császár G, Daurer A (eds) *Jubiläumsschrift 20 Jahre Geologischen Zusammenarbeit Österreich-Ungarn Lobitzer*, 55–72
- Balogh K, Itaya T, Németh K, Martin U, Wijbrans J, Thanh NX (2005) Study of controversial K/Ar and <sup>40</sup>Ar/<sup>39</sup>Ar ages of the Pliocene alkali basalt of Hegyestű, Balaton Highland, Hungary: a progress report. *Mineralia Slovaca* 37:298–300
- Barnes SJ, Roeder PL (2001) The range of spinel compositions in terrestrial mafic and ultramafic rocks. *J Petrol* 42:2279–2302
- Barruol G, Bonnin M, Pedersen H, Bokelmann GHR, Tiberi C (2011) Belt-parallel mantle flow beneath a halted continental collision: the Western Alps. *Earth Planet Sci Lett* 302:429–438
- Beccaluva L, Bianchini G, Bonadiman C, Coltorti M, Milani L, Salvini L, Siena F, Tassinari R (2007) Intraplate lithospheric and sub-lithospheric components in the Adriatic domain: nephelinite to tholeiite magma generation in the Paleogene Veneto Volcanic Province, Southern Alps. In: Beccaluva L, Bianchini G, Wilson M (eds) *Cenozoic Volcanism in the Mediterranean Area: Geological Society of America, special paper* 418:131–152
- Beccaluva L, Bianchini G, Natali C, Siena F (2011) Geodynamic control on orogenic and anorogenic magmatic phases in Sardinia and Southern Spain: inferences for the Cenozoic evolution of the western Mediterranean. *Lithos* 123:218–224
- Bianchini G, Beccaluva L, Siena F (2008) Postcollisional and intraplate Cenozoic volcanism in the rifted Apennines/Adriatic domain. *Lithos* 101:125–140
- Blondes MS, Reiners PW, Ducea MN, Singer BS, Chesley J (2008) Temporal-compositional trends over short and long time-scales

- in basalts of the Big Pine Volcanic Field, California. *Earth Planet Sci Lett* 269:140–154
- Borsy Z, Balogh K, Kozák M, Pécskay Z (1986) Újabb adatok a Tapolcai-medence fejlődéstörténetéhez. *Acta Geographica Debrecina* 23:79–104
- Bradshaw TK, Hawkesworth CJ, Gallagher K (1993) Basaltic volcanism in the Southern Basin and Range: no role for a mantle plume. *Earth Planet Sci Lett* 116:45–62
- Brenna M, Cronin SJ, Smith IEM, Sohn YK, Németh K (2010) Mechanisms driving polymagmatic activity at a monogenetic volcano, Udo, Jeju Island, South Korea. *Contrib Mineral Petrol* 160:931–950
- Brenna M, Cronin SJ, Smith IEM, Maas R, Sohn YK (2012) How small-volume basaltic magmatic systems develop: a case study from the Jeju Island Volcanic Field, Korea. *J Petrol* 53:985–1018
- Buikink A, Trieloff M, Hopp J, Althaus T, Korochantseva E, Schwarz WH, Altherr R (2005) Noble gas isotopes suggest deep mantle plume source of late Cenozoic mafic alkaline volcanism in Europe. *Earth Planet Sci Lett* 230:143–162
- Burov E, Cloetingh S (2009) Controls of mantle plumes and lithospheric folding on modes of intraplate continental tectonics: differences and similarities. *Geophys J Int* 178:1691–1722
- Cebriá JM, Wilson M (1995) Cenozoic mafic magmatism in western/central Europe: a common European asthenospheric reservoir? *Terra Nova* 7:162
- Cebriá JM, López-Ruiz J (1995) Alkali basalts and leucitites in an extensional intracontinental plate setting: the late Cenozoic Calatrava Volcanic Province (central Spain). *Lithos* 35:27–46
- Chaffey DJ, Cliff RA, Wilson BM (1989) Characterization of the St. Helena magma source. In: Saunders AD, Norry MJ (eds) *Magmatism in the Ocean Basins*. Geological Society Special Publication 42:257–276
- Chernyshev IV, Konečný V, Lexa J, Kovalenker VA, Jeleň S, Lebedev VA, Goltzman YV (2013) K–Ar and Rb–Sr geochronology and evolution of the Štiavica Stratovolcano (Central Slovakia). *Geol Carpath* 64:327–351
- Class C, Goldstein SL (1997) Plume–lithosphere interactions in the ocean basins: constraints from the source mineralogy. *Earth Planet Sci Lett* 150:245–260
- Cloetingh SAPL, Ziegler PA, Bogaard PJF, Andriessen PAM, Artemieva IM, Bada G, Balen RT, Beekman F, Ben-Avraham Z, Brun JP, Bunge HP, Burov EB, Carbonell R, Facenna C, Friedrich A, Gallart J, Green AG, Heidbach O, Jones AG, Matenco L, Mosar J, Oncken O, Pascal C, Peters G, Šliaupa S, Soesoo A, Spakman W, Stephenson RA, Thybo H, Torsvik T, de Vicente G, Wenzel F, Wortel MJR, TOPO-EUROPE Working Group 2 (2007) TOPO-EUROPE: the geoscience of coupled deep Earth-surface processes. *Glob Planet Chang* 58:1–118
- Clyne MA, Borg LE (1997) Olivine and chromian spinel in primitive calc-alkaline and tholeiitic lavas from the southernmost Cascade Range, California: a reflection of relative fertility of the source. *Can Mineral* 35:453–472
- Condit CD, Connor CB (1996) Recurrence rates of volcanism in basaltic volcanic fields: an example from the Springerville volcanic field, Arizona. *Geol Soc Am Bull* 108:1225–1241
- Connor CB, Conway FM (2000) Basaltic Volcanic Fields. In: Sigurdsson H (ed) *Encyclopedia of Volcanoes*. Academic Press, San Diego, pp 331–343
- Courtillot V, Davaille A, Besse J, Stock J (2003) Three distinct types of hotspots in the Earth's mantle. *Earth Planet Sci Lett* 205:295–308
- Csontos L, Nagymarosy A, Horváth F, Kovács M (1992) Tertiary evolution of the intra-Carpathian area: a model. *Tectonophysics* 208:221–241
- Dando BDE, Stuart GW, Houseman GA, Hegedűs E, Brückl E, Radovanovic S (2011) Teleseismic tomography of the mantle in the Carpathian–Pannonian region of central Europe. *Geophys J Int* 186:11–31
- Dasgupta R, Hirschmann MM, Stalker K (2006) Immiscible transition from carbonate-rich to silicate-rich melts in the 3 GPa melting interval of eclogite + CO<sub>2</sub> and genesis of silica-undersaturated ocean island lavas. *J Petrol* 47:647–671
- Dasgupta R, Jackson MG, Lee CTA (2010) Major element chemistry of ocean island basalts—conditions of mantle melting and heterogeneity of mantle source. *Earth Planet Sci Lett* 289:377–392
- DePaolo DJ, Daley EE (2000) Neodymium isotopes in basalts of the southwest basin and range and lithospheric thinning during continental extension. *Chem Geol* 169:157–185
- Dérerova J, Zeyen H, Bielik M, Salman K (2006) Application of integrated geophysical modeling for determination of the continental lithospheric thermal structure in the eastern Carpathians. *Tectonics* 25:TC3009. doi:10.1029/2005TC001883
- Dick HJB, Bullen T (1984) Chromian spinel as a petrogenetic indicator in abyssal and alpine-type peridotites and spatially associated lavas. *Contrib Miner Petrol* 86:54–76
- Dobosi G (1989) Clinopyroxene zoning patterns in the young alkali basalts of Hungary and their petrogenetic significance. *Contrib Miner Petrol* 101:112–121
- Dobosi G, Fodor RV (1992) Magma fractionation, replenishment, and mixing as inferred from green-core clinopyroxenes in Pliocene basanite, southern Slovakia. *Lithos* 28:133–150
- Dobosi G, Fodor RV, Goldberg SA (1995) Late-Cenozoic alkali basalt magmatism in Northern Hungary and Slovakia: petrology, source compositions and relationship to tectonics. *Acta Vulcanol* 7:199–207
- Dombrádi E, Sokoutis D, Bada G, Cloetingh S, Horváth F (2010) Modelling deformation of the Pannonian lithosphere: lithospheric folding and tectonic topography. *Tectonophysics* 484:103–118
- Downes H, Seghedi I, Szakács A, Dobosi G, James DE, Vaselli O, Rigby IJ, Ingram GA, Rex D, Pécskay Z (1995) Petrology and geochemistry of late Tertiary/Quaternary mafic alkaline volcanism in Romania. *Lithos* 35:65–81
- Ellam RM (1992) Lithospheric thickness as a control on basalt geochemistry. *Geology* 20:153–156
- Embey-Isztin A, Dobosi G (1995) Mantle source characteristics for Miocene–Pleistocene alkali basalts, Carpathian–Pannonian region: a review of trace elements and isotopic composition. *Acta Vulcanol* 7:155–166
- Embey-Isztin A, Dobosi G (2007) Composition of olivines in the young alkali basalts and their peridotite xenoliths from the Pannonian basin. *Annales Historico-Naturales Musei Nationalis Hungarici* 99:5–22
- Embey-Isztin A, Downes H, James DE, Upton BGC, Dobosi G, Ingram GA, Harmon RS, Scharbert HG (1993) The petrogenesis of Pliocene alkaline volcanic rocks from the Pannonian basin, Eastern Central Europe. *J Petrol* 34:317–343
- Embey-Isztin A, Dobosi G, Altherr R, Meyer HP (2001) Thermal evolution of the lithosphere beneath the western Pannonian basin: evidence from deep-seated xenoliths. *Tectonophysics* 331:285–306
- Erlund EJ, Cashman KV, Wallace PJ, Pioli L, Rosi M, Johnson E, Granados HD (2010) Compositional evolution of magma from Parícutin Volcano, Mexico: the tephra record. *J Volcanol Geotherm Res* 197:167–187
- Fekiacova Z, Mertz DF, Hofmann AW (2007) Geodynamic setting of the Tertiary Hocheifel volcanism (Germany), part II: geochemistry and Sr, Nd and Pb isotopic compositions. In: Ritter J, Christensen U (eds) *Mantle plumes—a multidisciplinary approach*. Springer, Berlin, pp 207–239
- Fisk MR, Bence AE (1980) Experimental crystallization of chrome spinel in FAMOUS basalt 527-1-1. *Earth Planet Sci Lett* 48:111–123

- Fitton JG, James D, Kempton PD, Ormerod DS, Leeman WP (1988) The role of lithospheric mantle in the generation of late Cenozoic basic magmas in the western United States. *J Petrol Spec* 1:331–349
- Fitton JG, James D, Leeman WP (1991) Basic magmatism associated with late Cenozoic extension in the western United States: compositional variations in space and time. *J Geophys Res* 96:13693–13711
- Gazel E, Plank T, Forsyth DW, Bendersky C, Lee C, Hauri E (2012) Lithosphere versus asthenosphere mantle sources at Big Pine Volcanic Field. *Geochem Geophys Geosyst* 13. doi:10.1029/2012GC004060
- Girbacea R, Frisch W, Linzer HG (1998) Post-orogenic uplift induced extension: a kinematic model for the Pliocene to recent tectonic evolution of the Eastern Carpathians (Romania). *Geol Carpath* 49:315–327
- Goes S, Spakman W, Bijwaard H (1999) A lower mantle source for central European volcanism. *Science* 286:1928–1931
- Granet M, Wilson M, Achauer U (1995) Imaging a mantle plume beneath the French Massif Central. *Earth Planet Sci Lett* 136:281–296
- Haase KM, Renno AD (2008) Variation of magma generation and mantle sources during continental rifting observed in Cenozoic lavas from the Eger Rift, Central Europe. *Chem Geol* 257:195–205
- Haase KM, Goldschmidt B, Garbe-Schönberg CD (2004) Petrogenesis of Tertiary continental intraplate lavas from the Westerwald region, Germany. *J Petrol* 45:883–905
- Halliday AN, Lee DC, Tommasini S, Davies GR, Paslick CR, Fitton JG, James DE (1995) Incompatible trace element in OIB and MORB source enrichment in the sub-oceanic mantle. *Earth Planet Sci Lett* 133:379–395
- Harangi S (2001a) Neogene to Quaternary volcanism of the Carpathian–Pannonian region: a review. *Acta Geol Hung* 44:223–258
- Harangi S (2001b) Neogene magmatism in the Alpine–Pannonian Transition zone: a model for melt generation in a complex geodynamic setting. *Acta Vulcanol* 13:1–11
- Harangi S (2009) Volcanism of the Carpathian–Pannonian region, Europe: the role of subduction, extension and mantle plumes. *MantlePlumes.org*, <http://www.mantleplumes.org/CarpathianPannonian.html>. Accessed 18 March 2014
- Harangi S, Lenkey L (2007) Genesis of the Neogene to Quaternary volcanism in the Carpathian–Pannonian region: role of subduction, extension, and mantle plume. *Geol Soc Am Spec Pap* 418:67–92
- Harangi S, Downes H, Thirlwall M, Gmélning K (2007) Geochemistry, petrogenesis and geodynamic relationships of Miocene calc-alkaline volcanic rocks in the Western Carpathian arc, eastern central Europe. *J Petrol* 48:2261–2287
- Harangi S, Vaselli O, Tonarini S, Szabó C, Harangi R, Coradossi N (1995) Petrogenesis of Neogene extension-related alkaline volcanic rocks of the Little Hungarian Plain volcanic field (Western Hungary). *Acta Vulcanol* 7:173–187
- Harangi S, Downes H, Seghedi I (2006) Tertiary–Quaternary subduction processes and related magmatism in the Alpine–Mediterranean region. In: Gee DG, Stephenson RA (eds) *European lithosphere dynamics*. *Geol Soc Lond Mem* 32:167–190
- Harangi S, Sági T, Seghedi I, Ntaflou T (2013) A combined whole-rock and mineral-scale investigation to reveal the origin of the basaltic magmas of the Perșani monogenetic volcanic field, Romania, eastern–central Europe. *Lithos* 180–181:43–57
- Hart SR (1988) Heterogeneous mantle domains: signatures, genesis and mixing chronologies. *Earth Planet Sci Lett* 90:273–296
- Herzberg C (2011) Identification of source lithology in the Hawaiian and Canary Islands: implications for origins. *J Petrol* 52:113–146
- Herzberg C, Asimow PD (2008) Petrology of some oceanic island basalts: PRIMELT2.XLS software for primary magma calculation. *Geochem Geophys Geosyst* 9:Q09001. doi:10.1029/2008GC002057
- Hetényi G, Stuart G, Houseman G, Horvath F, Hegedüs E, Brückl E (2009) Anomalous deep mantle transition zone below Central Europe: evidence of lithospheric instability. *Geophys Res Lett* 36. doi:10.1029/2009GL040171
- Hill R, Roeder P (1974) The crystallization of spinel from basaltic liquid as a function of oxygen fugacity. *J Geol* 82:709–729
- Hirose K, Kawamoto T (1995) Hydrous partial melting of lherzolite at 1 GPa: the effect of H<sub>2</sub>O on the genesis of basaltic magmas. *Earth Planet Sci Lett* 133:463–473
- Hirose K, Kushiro I (1993) Partial melting of dry peridotites at high pressures: determination of composition of melts segregated from peridotite using aggregate of diamonds. *Earth Planet Sci Lett* 114:477–489
- Hirschmann MM (2000) Mantle solidus: experimental constraints and the effects of peridotite composition. *Geochem Geophys Geosyst* 1:1042. doi:10.1029/2000GC000070
- Hirschmann MM (2006) Water, melting, and the deep Earth H<sub>2</sub>O cycle. *Annu Rev Earth Planet Sci* 34:629–653
- Hirschmann MM, Tenner T, Aubaud C, Withers AC (2009) Dehydration melting of nominally anhydrous mantle: the primacy of partitioning. *Phys Earth Planet Inter* 176:54–68
- Hoernle K, Zhang YS, Graham D (1995) Seismic and geochemical evidence for large-scale mantle upwelling beneath the eastern Atlantic and western and central Europe. *Nature* 374:34–39
- Horváth F (1993) Towards a mechanical model for the formation of the Pannonian basin. *Tectonophysics* 226:333–357
- Horváth F, Cloetingh S (1996) Stress-induced late-stage subsidence anomalies in the Pannonian basin. *Tectonophysics* 266:287–300
- Horváth F, Faccenna C (2011) Central Mediterranean mantle flow system and the formation of the Pannonian basin. *Geophys Res Abstr* 13:EGU2011-8894-2
- Horváth F, Dövényi P, Szalay Á, Royden LH (1988) Subsidence, thermal and maturation history of the Great Hungarian Plain. In: Royden LH, Horváth F (eds) *The Pannonian basin: a case study in basin evolution*. *AAPG Mem* 45:355–372
- Horváth F, Bada G, Szafián P, Tari G, Ádám A, Cloetingh S (2006) Formation and deformation of the Pannonian basin. In: Gee DG, Stephenson RA (eds) *European lithosphere dynamics*. *Geol Soc Lond Mem* 32:191–207
- Huismans RS, Podladchikov YY, Cloetingh S (2001) Dynamic modeling of the transition from passive to active rifting, application to the Pannonian basin. *Tectonics* 20:1021–1039
- Humphreys ER, Niu Y (2009) On the composition of ocean island basalts (OIB): the effects of lithospheric thickness variation and mantle metasomatism. *Lithos* 112:118–136
- Hurai V, Danišák M, Huraiová M, Paquette JL, Ádám A (2013) Combined U/Pb and (U-Th)/He geochronometry of basalt maars in Western Carpathians: implications for age of intraplate volcanism and origin of zircon metasomatism. *Contrib Mineral Petrol* 166:1235–1251
- Jankovics MÉ, Harangi S, Kiss B, Ntaflou T (2012) Open-system evolution of the Füzes-tó alkaline basaltic magma, western Pannonian basin: constraints from mineral textures and compositions. *Lithos* 140–141:25–37
- Jankovics MÉ, Dobosi G, Embey-Isztin A, Kiss B, Sági T, Harangi S, Ntaflou T (2013) Origin and ascent history of unusually crystal-rich alkaline basaltic magmas from the western Pannonian basin. *Bull Volcanol* 75:1–23

- Jung C, Jung S, Hoffer E, Berndt J (2006) Petrogenesis of Tertiary mafic alkaline magmas in the Hoheifel, Germany. *J Petrol* 47:1637–1671
- Jung S, Pfänder JA, Brüggemann G, Stracke A (2005) Sources of primitive alkaline rocks from the Central European Volcanic Province (Rhön, Germany) inferred from Hf, Os and Pb isotopes. *Contrib Miner Petrol* 150:546–559
- Jung S, Vieten K, Romer RL, Mezger K, Hoernes S, Satir M (2012) Petrogenesis of Tertiary alkaline magmas in the Siebengebirge, Germany. *J Petrol* 53:2381–2409
- Kamenetsky VS, Crawford AJ, Meffre S (2001) Factors controlling chemistry of magmatic spinel: an empirical study of associated olivine, Cr-spinel and melt inclusions from primitive rocks. *J Petrol* 42:655–671
- Karato S (2011) Water distribution across the mantle transition zone and its implications for the global material circulation. *Earth Planet Sci Lett* 301:413–423
- Kawabata H, Hanyu T, Chang Q, Kimura JI, Nichols ARL, Tatsumi Y (2011) The petrology and geochemistry of St. Helena alkali basalts: evaluation of the oceanic crust-recycling model for HIMU OIB. *J Petrol* 52:791–838
- Kereszturi G, Németh K, Csillag G, Balogh K, Kovács J (2011) The role of external environmental factors in changing eruption styles of monogenetic volcanoes in a Mio/Pleistocene continental volcanic field in western Hungary. *J Volcanol Geotherm Res* 201:227–240
- Kereszturi G, Németh K, Lexa J, Konečný V, Pécskay Z (2013) Eruptive volume estimate of the Nógrád-Gömör/Novohrad-Gemer volcanic field (Slovakia–Hungary). In: Buecher J, Rappich V, Tietz O (eds) Abstract volume and excursion guides—basalt 2013:168–169
- Klemme S, O'Neill HSC (2000) The near-solidus transition from garnet lherzolite to spinel lherzolite. *Contrib Miner Petrol* 138:237–248
- Klemme S (2004) The influence of Cr on the garnet–spinel transition in the Earth's mantle: experiments in the system MgO–Cr<sub>2</sub>O<sub>3</sub>–SiO<sub>2</sub> and thermodynamic modelling. *Lithos* 77:639–646
- Kogiso T, Hirschmann MM, Frost DJ (2003) High-pressure partial melting of garnet pyroxenite: possible mafic lithologies in the source of ocean island basalts. *Earth Planet Sci Lett* 216:603–617
- Kogiso T, Hirschmann MM (2006) Partial melting experiments of biminerally eclogite and the role of recycled mafic oceanic crust in the genesis of ocean island basalts. *Earth Planet Sci Lett* 249:188–199
- Konečný V, Lexa J, Balogh K, Konečný P (1995) Alkali basalt volcanism in Southern Slovakia: volcanic forms and time evolution. *Acta Volcanol* 7:167–171
- Konečný V, Lexa J, Balogh K (1999) Neogene–Quaternary alkali basalt volcanism in Central and Southern Slovakia (Western Carpathians). *Geolines* 9:67–75
- Konečný V, Kováč M, Lexa J, Šefara J (2002) Neogene evolution of the Carpatho–Pannonian region: an interplay of subduction and back-arc diapiric uprising in the mantle. *EGU Stephan Mueller Spec Publ Ser* 1:105–123
- Kostopoulos DK, James SD (1992) Parameterization of the melting regime of the shallow upper mantle and the effects of variable lithospheric stretching on mantle modal stratification and trace element concentrations in magmas. *J Petrol* 33:665–691
- Kovács I, Falus G, Stuart G, Hidas K, Szabó C, Flower MFJ, Hegedűs E, Posgay K, Zilahi-Sebess L (2012) Seismic anisotropy and deformation patterns in upper mantle xenoliths from the central Carpathian–Pannonian region: asthenospheric flow as a driving force for Cenozoic extension and extrusion? *Tectonophysics* 514–517:168–179
- Langmuir CH, Forsyth DW (2007) Mantle melting beneath mid-ocean ridges. *Oceanography* 20:78–89
- Langmuir CH, Klein E, Plank T (1992) Petrological systematics of mid-ocean ridge basalts: constraints on melt generation beneath ocean ridges. *AGU Monogr* 71:183–280
- Le Bas MJ, Le Maitre RW, Streckeisen A, Zanettin B (1986) A chemical classification of volcanic rocks based on the total alkali–silica diagram. *J Petrol* 27(745):750
- Lebedev S, Meier T, van der Hilst RD (2006) Asthenospheric flow and origin of volcanism in the Baikal Rift area. *Earth Planet Sci Lett* 249:415–424
- Lee CT, Luffi P, Plank T, Dalton H, Leeman WP (2009) Constraints on the depths and temperatures of basaltic magma generation on Earth and other terrestrial planets using new thermobarometers for mafic magmas. *Earth Planet Sci Lett* 279:20–33
- Leloup PH, Lacassin R, Tapponnier P, Schärer U, Dalai Z, Xiaohan L, Liangshang Z, Shaocheng J, Trinh PT (1995) The Ailao Shan–Red River shear zone (Yunnan, China), Tertiary transform boundary of Indochina. *Tectonophysics* 251:3–84
- Lenkey L, Dövényi P, Horváth F, Cloetingh S (2002) Geothermics of the Pannonian basin and its bearing on the neotectonics. *Eur Geophys Union Stephan Mueller Spec Publ Ser* 3:29–40
- Lexa J, Seghedi I, Németh K, Szakács A, Konečný V, Pécskay Z, Fülöp A, Kovacs M (2010) Neogene–Quaternary volcanic forms in the Carpathian–Pannonian region: a review. *Cent Eur J Geosci* 2:207–270
- Lorinczi P, Houseman GA (2009) Lithospheric gravitational instability beneath the Southeast Carpathians. *Tectonophysics* 474:322–336
- Luhr JF, Carmichael ISE (1985) Jorullo volcano, Michoacán, Mexico (1759–1774): the earlier stages of fractionation in calc-alkaline magmas. *Contrib Miner Petrol* 90:142–161
- Lustrino M, Wilson M (2007) The circum-Mediterranean anorogenic Cenozoic igneous province. *Earth Sci Rev* 81:1–65
- Ma GSK, Malpas J, Xenophontos C, Chan GHN (2011) Petrogenesis of latest Miocene–Quaternary continental intraplate volcanism along the northern Dead Sea Fault System (Al Ghab–Homs volcanic field), western Syria: evidence for lithosphere–asthenosphere interaction. *J Petrol* 52:401–430
- Martin U, Németh K (2004) Mio/Pliocene phreatomagmatic volcanism in the western Pannonian basin. *Geological Institute of Hungary, Budapest*
- Martin M, Wenzel F, CALIXTO Working Group (2006) High-resolution teleseismic body wave tomography beneath SE Romania: II. Imaging of a slab detachment scenario. *Geophys J Int* 164:579–595
- Mayer B, Jung S, Romer RL, Stracke A, Haase KM, Garbe-Schönberg CD (2013) Petrogenesis of Tertiary hornblende-bearing lavas in the Rhön, Germany. *J Petrol* 54:2095–2123
- Mayer B, Jung S, Romer R, Pfänder JA, Klügel A, Pack A, Gröner E (2014) Amphibole in alkaline basalts from intraplate settings: implications for the petrogenesis of alkaline lavas from the metasomatised lithospheric mantle. *Contrib Mineral Petrol* 167. doi:10.1007/s00410-014-0989-3
- McDonough WF, Sun SS (1995) The composition of the Earth. *Chem Geol* 120:223–253
- McGee LE, Millet MA, Smith IEM, Németh K, Lindsay JM (2012) The inception and progression of melting in a monogenetic eruption: Motukorea Volcano, the Auckland Volcanic Field, New Zealand. *Lithos* 155:360–374
- McGee LE, Smith IEM, Millet MA, Handley HK, Lindsay JM (2013) Asthenospheric control of melting processes in a monogenetic basaltic system: a case study of the Auckland Volcanic Field, New Zealand. *J Petrol* 54:2125–2153
- McKenzie D (1989) Some remarks on the movement of small melt fractions in the mantle. *Earth Planet Sci Lett* 95:53–72
- Niu Y (2005) Generation and evolution of basaltic magmas: some basic concepts and a hypothesis for the origin of the

- Mesozoic–Cenozoic volcanism in eastern China. *Geol J China Univ* 11:9–46
- Niu Y (2008) The origin of alkaline lavas. *Science* 320:883–884
- Niu Y, Wilson M, Humphreys ER, O'Hara MJ (2011) The origin of intra-plate ocean island basalts (OIB): the lid effect and its geodynamic implications. *J Petrol* 52:1443–1468
- Ormerod DS, Rogers NW, Hawkesworth CJ (1991) Melting in the lithospheric mantle: inverse modelling of alkali-olivine basalts from the Big Pine Volcanic Field, California. *Contrib Miner Petrol* 108:305–317
- Panaiotu CG, Jicha BR, Singer BS, Tugui A, Seghedi I, Panaiotu AG, Necula C (2013) <sup>40</sup>Ar/<sup>39</sup>Ar chronology and paleomagnetism of Quaternary basaltic lavas from the Perșani Mountains (East Carpathians). *Phys Earth Planet Inter* 221:1–24
- Panaiotu CG, Pécskay Z, Hambach U, Seghedi I, Panaiotu CE, Tetsumaru I, Orleanu M, Szakács A (2004) Short-lived Quaternary volcanism in the Persani Mountains (Romania) revealed by combined K–Ar and paleomagnetic data. *Geol Carpath* 55:333–339
- Pécskay Z, Lexa J, Szakács A, Seghedi I, Balogh K, Konečný V, Zelenka T, Kovacs M, Póka T, Fülöp A, Márton E, Panaiotu C, Cvetković V (2006) Geochronology of Neogene–Quaternary magmatism in the Carpathian arc and Intra-Carpathian area: a review. *Geol Carpath* 57:511–530
- Pertermann M, Hirschmann MM (2003) Partial melting experiments on a MORB-like pyroxenite between 2 and 3 GPa: constraints on the presence of pyroxenite in basalt source regions from solidus location and melting rate. *J Geophys Res: Solid Earth* 108(B2):2125. doi:10.1029/2000JB000118
- Pilet S, Hernandez J, Sylvester P, Poujol M (2005) The metasomatic alternative for ocean island basalt chemical heterogeneity. *Earth Planet Sci Lett* 236:148–166
- Pilet S, Baker MB, Stolper EM (2008) Metasomatized lithosphere and the origin of alkaline lavas. *Science* 320:916–919
- Piomallo C, Morelli A (2003) P wave tomography of the mantle under the Alpine-Mediterranean area. *J Geophys Res* 108. doi:10.1029/2002JB001757
- Piomallo C, Vincent AP, Yuen DA, Morelli A (2001) Dynamics of the transition zone under Europe inferred from wavelet cross-spectra of seismic tomography. *Phys Earth Planet Inter* 125:125–139
- Popa M, Radulian M, Szakács A, Seghedi I, Zaharia B (2012) New seismic and tomography data in the southern part of the Harghita Mountains (Romania, Southeastern Carpathians): connection with recent volcanic activity. *Pure appl Geophys* 169:1557–1573
- Putirka K (1999) Melting depths and mantle heterogeneity beneath Hawaii and the East Pacific Rise: constraints from Na/Ti and rare earth element ratios. *J Geophys Res* 104:2817–2829
- Robinson JA, Wood BJ (1998) The depth of the spinel to garnet transition at the peridotite solidus. *Earth Planet Sci Lett* 164:277–284
- Roeder PL, Reynolds I (1991) Crystallization of chromite and chromium solubility in basaltic melts. *J Petrol* 32:909–934
- Roeder PL, Thornber C, Poustovetov A, Grant A (2003) Morphology and composition of spinel in Pu'u 'O'o lava (1996–1998), Kilauea volcano, Hawaii. *J Volcanol Geotherm Res* 123:245–265
- Roeder P, Gofton E, Thornber C (2006) Cotectic proportions of olivine and spinel in olivine–tholeiitic basalt and evaluation of pre-eruptive processes. *J Petrol* 47:883–900
- Royden LH, Horváth F, Burchfiel BC (1982) Transform faulting, extension and subduction in the Carpathian–Pannonian region. *Geol Soc Am Bull* 93:717–725
- Rudnick RL, Fountain DM (1995) Nature and composition of the continental crust: a lower crustal perspective. *Rev Geophys* 33:267–309
- Sági T, Harangi S (2013) Origin of the magmas in the Late Miocene to Quaternary Nógrád-Selmec monogenetic alkali basalt volcanic field, southern–central Slovakia. In: Büchner J, Rapprich V, Tietz O (eds) Basalt 2013 conference abstract and excursion guides. Görlitz, Germany, pp 17–18
- Sakuyama T, Ozawa K, Sumino H, Nagao K (2009) Progressive melt extraction from upwelling mantle constrained by the Kita–Matsura Basalts in NW Kyushu, SW Japan. *J Petrol* 50:725–779
- Salter VJM, Hart SR (1989) The hafnium paradox and the role of garnet in the source of mid-ocean-ridge basalts. *342:420–422*
- Salter VJM, Stracke A (2004) Composition of the depleted mantle. *Geochem Geophys Geosyst* 5:Q05B07. doi:10.1029/2003GC000597
- Scarow JH, Cox KG (1995) Basalts generated by decompressive adiabatic melting of a mantle plume: a case study from the Isle of Skye, NW Scotland. *J Petrol* 36:3–22
- Sclater J, Royden L, Horváth F, Burchfiel B, Semken S, Stegena L (1980) The formation of the intra-Carpathian basins as determined from subsidence data. *Earth Planet Sci Lett* 51:139–162
- Seghedi I, Szakács A (1994) The upper Pliocene–Pleistocene effusive and explosive basaltic volcanism from the Perșani Mountains. *Rom J Petrol* 76:101–107
- Seghedi I, Downes H (2011) Geochemistry and tectonic development of Cenozoic magmatism in the Carpathian–Pannonian region. *Gondwana Res* 20:655–672
- Seghedi I, Balintoni I, Szakács A (1998) Interplay of tectonics and neogene post-collisional magmatism in the intracarpathian region. *Lithos* 45:483–497
- Seghedi I, Downes H, Szakács A, Mason PRD, Thirlwall MF, Rosu E, Pécskay Z, Marton E, Panaiotu C (2004a) Neogene–Quaternary magmatism and geodynamics in the Carpathian–Pannonian region: a synthesis. *Lithos* 72:117–146
- Seghedi I, Downes H, Vaselli O, Szakács A, Balogh K, Pécskay Z (2004b) Post-collisional Tertiary–Quaternary mafic alkalic magmatism in the Carpathian–Pannonian region: a review. *Tectonophysics* 393:43–62
- Seghedi I, Downes H, Harangi S, Mason PRD, Pécskay Z (2005) Geochemical response of magmas to Neogene–Quaternary continental collision in the Carpathian–Pannonian region: a review. *Tectonophysics* 410:485–499
- Seghedi I, Mañenco L, Downes H, Mason PRD, Szakács A, Pécskay Z (2011) Tectonic significance of changes in post-subduction Pliocene–Quaternary magmatism in the south east part of the Carpathian–Pannonian region. *Tectonophysics* 502:146–157
- Shaw DM (1970) Trace element fractionation during anatexis. *Geochim Cosmochim Acta* 34:237–243
- Shaw DM (2000) Continuous (dynamic) melting theory revisited. *Can Mineral* 38:1041–1063
- Sigurdsson H, Schilling JG (1976) Spinels in mid-atlantic ridge basalts: chemistry and occurrence. *Earth Planet Sci Lett* 29:7–20
- Šimon L, Halouzka R (1996) Pútkov vršok volcano: the youngest volcano in the Western Carpathians. *Slovak Geol Mag* 2:103–123
- Šimon L, Maglay J (2005) Dating of sediments underlying the Putikov vršok volcano lava flow by the OSL method. *Miner Slovaca* 37:279–281
- Smith IEM, Blake S, Wilson CJN, Houghton BF (2008) Deep-seated fractionation during the rise of a small-volume basalt magma batch: Crater Hill, Auckland, New Zealand. *Contrib Miner Petrol* 155:511–527
- Sobolev AV, Shimizu N (1992) Ultradepleted melts and the permeability of the oceanic mantle. *Dokl Ross Akad Nauk* 326:354–360
- Sobolev AV, Hofmann AW, Sobolev SV, Nikogosian IK (2005) An olivine-free mantle source of Hawaiian shield basalts. *Nature* 434:590–597
- Sobolev AV, Hofmann AW, Kuzmin DV, Yaxley GM, Arndt NT, Chung SL, Danyushevsky LV, Elliott T, Frey FA, Garcia MO,

- Gurenko AA, Kamenetsky VS, Kerr AC, Krivolutsкая NA, Matvienkov VV, Nikogosian IK, Rocholl A, Sigurdsson IA, Sushchevskaya NM, Teklay M (2007) The amount of recycled crust in sources of mantle-derived melts. *Science* 316:412–417
- Späth A, Le Roex AP, Opiyo-Akech N (2001) Plume–lithosphere interaction and the origin of continental rift-related alkaline volcanism—the Chyulu Hills Volcanic Province, Southern Kenya. *J Petrol* 42:765–787
- Sperner B, Lorenz F, Bonjer K, Hettel S, Muller B, Wenzel F (2001) Slab break-off: abrupt cut or gradual detachment? New insights from the Vrancea Region (SE Carpathians, Romania). *Terra Nova* 13:172–179
- Sperner B, Ioane D, Lillie RJ (2004) Slab behaviour and its surface expression: new insights from gravity modelling in the SE-Carpathians. *Tectonophysics* 382:51–84
- Stegena L, Géczy B, Horváth F (1975) Late Cenozoic evolution of the Pannonian basin. *Tectonophysics* 26:71–90
- Stracke A, Hofmann AW, Hart SR (2005) FOZO, HIMU and the rest of the mantle zoo. *Geochem Geophys Geosyst* 6. doi:10.1029/2004GC000824
- Strong M, Wolff J (2003) Compositional variations within scoria cones. *Geology* 31:143–146
- Sun S, McDonough WF (1989) Chemical and isotopic systematics of oceanic basalts: implications for mantle compositions and processes. *Geol Soc Spec Pub* 42:313–345
- Szabó C, Harangi S, Csontos L (1992) Review of neogene and quaternary volcanism of the Carpathian–Pannonian region. *Tectonophysics* 208:243–256
- Szabó C, Falus G, Zajacz Z, Kovács I, Bali E (2004) Composition and evolution of lithosphere beneath the Carpathian–Pannonian region: a review. *Tectonophysics* 393:119–137
- Takahashi E, Kushiro I (1983) Melting of a dry peridotite at high pressures and basalt magma genesis. *Am Mineral* 68:859–879
- Tari G, Dövényi P, Horváth F, Dunkl I, Lenkey L, Stefanescu M, Szafián P, Tóth T (1999). Lithospheric structure of the Pannonian basin derived from seismic, gravity and geothermal data. In: Durand B, Jolivet L, Horváth F, Séranne M (eds) *The Mediterranean basins: Tertiary extension within the Alpine orogen*. *Geol Soc Lond Spec Publ* 156:215–250
- Timm C, Hoernle K, van den Bogaard P, Bindeman I, Weaver S (2009) Geochemical evolution of intraplate volcanism at Banks Peninsula, New Zealand: interaction between asthenospheric and lithospheric melts. *J Petrol* 50:989–1023
- Timm C, Hoernle K, Werner R, Hauff F, van den Bogaard P, White J, Mortimer N, Garbe-Schönberg D (2010) Temporal and geochemical evolution of the Cenozoic intraplate volcanism of Zealandia. *Earth Sci Rev* 98:38–64
- Tschegg C, Ntaflou T, Kiraly F, Harangi S (2010) High temperature corrosion of olivine phenocrysts in Pliocene basalts from Banat, Romania. *Aust J Earth-Sci* 103:101–110
- Valentine GA, Perry FV (2007) Tectonically controlled, time-predictable basaltic volcanism from a lithospheric mantle source (central Basin and Range Province, USA). *Earth Planet Sci Lett* 261:201–216
- Vauchez A, Tommasi A, Mainprice D (2012) Faults (shear zones) in the Earth's mantle. *Tectonophysics* 558–559:1–27
- Wallace M, Green DH (1991) The effect of bulk rock composition on the stability of amphibole in the upper mantle: implications for solidus positions and mantle metasomatism. *Mineral Petrol* 44:1–19
- Walter MJ (1998) Melting of garnet peridotite and the origin of komatiite and depleted lithosphere. *J Petrol* 39:29–60
- Wang K, Plank T, Walker JD, Smith EI (2002) A mantle melting profile across the Basin and Range, SW USA. *J Geophys Res: Solid Earth* 107(1):ECV 5-1–ECV 5-21
- Wijbrans J, Németh K, Martin U, Balogh K (2007) 40Ar/39Ar geochronology of Neogene phreatomagmatic volcanism in the western Pannonian basin, Hungary. *J Volcanol Geotherm Res* 164:193–204
- Wilson M, Bianchini G (1999) Tertiary–Quaternary magmatism within the Mediterranean and surrounding regions. In: Durand B, Jolivet L, Horváth F, Séranne M (eds) *The Mediterranean basins: Tertiary extension within the Alpine orogen*. *Geol Soc Lond Spec Publ* 156:141–168
- Wilson M, Downes H (1991) Tertiary–Quaternary extension-related alkaline magmatism in Western and Central Europe. *J Petrol* 32:811–849
- Wilson M, Downes H (2006) Tertiary–Quaternary intra-plate magmatism in Europe and its relationship to mantle dynamics. In: Stephenson R, Gee D (eds) *European lithosphere dynamics*. *Geol Soc Lond Mem* 32:147–166
- Wilson M, Patterson R. (2001) Intraplate magmatism related to short-wavelength convective instabilities in the upper mantle: evidence from the Tertiary–Quaternary volcanic province of western and central Europe. In: Ernst RE, Buchan KL (eds) *Mantle plumes: their identification through time*. *Geol Soc Am. Spec Pap* 352:37–58
- Woodland AB, Jugo PJ (2007) A complex magmatic system beneath the Devés volcanic field, Massif Central, France: evidence from clinopyroxene megacrysts. *Contrib Miner Petrol* 153:719–731
- Wortel MJR, Spakman W (2000) Subduction and slab detachment in the Mediterranean–Carpathian region. *Science* 290:1910–1917
- Zou H (1998) Trace element fractionation during modal and non-modal dynamic melting and open-system melting; a mathematical treatment. *Geochim Cosmochim Acta* 62:1937–1945